# ASSESSMENT OF CRACK KINEMATICS IN CONCRETE BEAMS USING DIGITAL IMAGE **CORRELATION**

Ву

Gabriela I. Zárate Garnica

in partial fulfillment of the requirements for the degree of

**Master of Science** in Structural Engineering

at the Delft University of Technology,

Student number: 4623363
Supervisor: Dr. ir. Y. Yang, TU Delft
Thesis committee: Dr. ir. M.A.N. Hendriks, TU Delft





# **CONTENTS**

	LIST OF FIGURES	4
	LIST OF TABLES	5
1.	. INTRODUCTION	6
	1.1. BACKGROUND AND MOTIVATION	
_	1.2 OBJECTIVES	
2.	LITERATURE REVIEW2.1 CRITICAL SHEAR DISPLACEMENT THEORY	8 8
	2.1.1 INTRODUCTION	
	2.2 MODEL-BASED ON A CRITICAL SHEAR DISPLACEMENT	10
	2.2.1 SIMPLIFIED CRACK PATTERN	10
	2.2.2 SIMPLIFIED SHEAR FORCE-DISPLACEMENT RELATIONSHIP	<sup>2</sup> 12
	2.3 CRITICAL SHEAR DISPLACEMENT	12
	2.4 EVALUATION OF THE SHEAR CAPACITY BASED ON THE CRITIC SHEAR DISPLACEMENT	
	2.5 CRACK WIDTH LIMIT ON AGGREGATE INTERLOCK	
3.	EXPERIMENTAL PROCEDURE	16
	3.1 SPECIMENS AND TEST SET UP	
,	3.2 DIGITAL IMAGE CORRELATION MEASUREMENTS	
4.	4.3 GENERAL APPROACH	
	4.4 DESCRIPTION OF RESULTS	
	4.5 DISCUSSION	
5.		
A. B.		
О.	B.1 RESULTS P502A2	
	B.1.1 LOADING SCHEME P502A2	50
	B.1.2 DIC RESULTS P502A2	50
	B.1.3 MEASURED HORIZONTAL DEFORMATIONS P502A2	52
	B.1.4 CRACK WIDTH ( $\Delta_x$ ) AND SHEAR DISPLACEMENT ( $\Delta_y$ ) P502A2	53
	B.2 RESULTS P804A1	56
	B.2.1 LOADING SCHEME P804A1	56
	B.2.2 DIC RESULTS P804A1	
	b.2.3 MEASURED HORIZONTAL DEFORMATIONS P804A1	59
	B.2.4 CRACK WIDTH ( $\Delta_x$ ) AND SHEAR DISPLACEMENT ( $\Delta_y$ ) P804A1	60
	B.3 RESULTS P804A2	64
	B.3.1 LOADING SCHEME P804A2	
	B.3.2 DIC RESULTS P804A2	
	B.3.3 MEASURED HORIZONTAL DEFORMATIONS P804A2	
	B.3.4 CRACK WIDTH ( $\Delta_x$ ) AND SHEAR DISPLACEMENT ( $\Delta_y$ ) P804A2	67

# LIST OF FIGURES

Figure 2.1 Free body of a flexural shear crack [9]	
Figure 2.2 Cracked sections with respect to their location [9]	9
Figure 2.3 Free body diagram with shear transfer mechanism [1]	.10
Figure 2.4 Simplified crack profile [1]	.11
Figure 2.5 Calculated critical shear displacement against effective height [6]	.13
Figure 2.6 Flow chart of the evaluation of the shear capacity based on critical shear	
displacement	.14
Figure 3.1 Reinforcement Layout. [5]	. 17
Figure 3.2 Configuration of the tests. [5]	
Figure 3.3 Typical LVDT's array	
Figure 3.4 Typical DIC painted pattern	
Figure 4.1 Main aspects of the general approach	
Figure 4.2 Steps for a typical correlation using the Matlab-based DIC code	
Figure 4.3 Procedure to obtain vertical and horizontal displacements	
Figure 4.4 Procedure to obtain the critical shear displacement, critical load and crack	
width	
Figure 4.5 Loading scheme for P804B1	
Figure 4.6 DIC results for representative load levels for P804B1	
Figure 4.7 LVDTs array location for P04B1	
Figure 4.8 Comparative of the horizontal deformation development of LVDT's 5-8 &	
DIC (bottom row) for P804B1	.25
Figure 4.9 Crack identification and location of the tensile reinforcement for P804B1.	
Figure 4.10 Shear displacement for major cracks for P804B1	
Figure 4.11 Shear displacement for secondary cracks for P804B1	
Figure 4.12 Critical inclined cracks and critical shear displacement for P804B1	
Figure 4.13 Crack width for major cracks P804B1	
Figure 4.14 Crack width for secondary cracks P804B1	
Figure 4.15 Crack width for Crack 1 for P804B1	
Figure 4.17 LVDTs vs DIC measurements for all test	
Figure 4.18 Crack identification	31
Tigaro 1. To Oraok Idonamodaoi	
Figure A.1 Main GUIs	35
Figure A.2 reference_UC	
Figure A.3 Example of RGB values	
Figure A.4 Area containing the red points	
Figure A.5 Marking of the horizontal edge of the specimen	
Figure A.6 Angle and scale	
Figure A.7 UC_Params photo parameters	
Figure A.8 Correlation Parameters for reduced images	
Figure A.9 Options for visualizing the reduced data	
Figure A.10 Options to view the contour plot	
Figure A.11 Correlation Parameters for full images	
Figure A.12 Options for visualizing full data	
Figure A.13 Options to view the contour plots	
Figure A.14 Compute data parameters	
Figure A.15 Options for visualizing the strains	
Figure A.16 Options to view the strains contour plot	
Figure A.17 Parameters for the filtering of images	
Figure A. 17 Farameters for the filtering of images	
Figure A. 19 UC_Cracks functions and tests	
Figure A.20 Example of W (crack width)	
Figure A.21 Example of W (crack width)	
I IYUIT ALL I LAAIIIPIE UI DEILA	. <del>4</del> 0

Figure A.22 GZ_Displ	. 48
Figure B.1 Loading scheme for P502A2	.50
Figure B.2 DIC results for P502A2	.52
Figure B.3 LVDTs array location for P502A2	.52
Figure B.4 Comparative of the horizontal deformation development of LVDT's 5-8 &	
DIC (bottom row) for P502A2	
Figure B.5 Crack identification and location of tensile reinforcement for P502A2	.54
Figure B.6 Shear displacement for major cracks for P502A2	
Figure B.7 Critical inclined cracks and critical shear displacement for P502A2	. 55
Figure B.8 Crack width for major cracks for P502A2	
Figure B.9 Crack width for Crack 1 P502A2	.55
Figure B.10 Loading scheme for P804A1	.56
Figure B.11 DIC results for representative load levels for P804A1-1 (First part)	
Figure B.12 DIC results for representative load levels P804A1-2 (Second part)	
Figure B.13 LVDTs array location for P804A1	
Figure B.14 Comparative of the horizontal deformation developments of LVDT's 5-8	&
DIC (bottom row) for P804A1	.60
Figure B.15 Crack identification and location of the tensile reinforcement for P804A1	61
Figure B.16 Shear displacement for major cracks for P804A1	
Figure B.17 Shear displacement for flexural cracks for P804A1	.62
Figure B.18 Critical cracks and critical shear displacement for P804A1	.62
Figure B.19 Crack width for major cracks for P804A1	.63
Figure B.20 Crack width for secondary cracks for P804A1	.63
Figure B.21 Crack width for Crack 1 P804A1	
Figure B.22 Loading scheme for P804A2	
Figure B.23 DIC results for representative load levels P804A2	.65
Figure B.24 LVDT array location for P804A2	.66
Figure B.25 Comparative of the horizontal deformation development of LVDT's 5-8 8	, X
DIC (bottom row) for P804A2	.66
Figure B.26 Crack identification and location of tensile reinforcement for P804A2	.67
Figure B.27 Shear displacement for major cracks for P804A2	.68
Figure B.28 Shear displacement for secondary cracks for P804A2	.68
Figure B.29 Critical cracks and critical shear displacement	
Figure B.30 Crack width for major cracks P804A2	.69
Figure B.31 Crack width for secondary cracks P804A2	.69
Figure B.32 Crack width for Crack 1 P804A2	.69
LIST OF TABLES	
	16
Table 1 Beams Properties Table 2 DIC parameters	
Table 3 Crack identification for all beams	
Table 3 Crack identification for all beams	
Table 4 Clack kinematics for all beams	. ou

# INTRODUCTION

### 1.1. BACKGROUND AND MOTIVATION

Shear in reinforced concrete beams is considered as one of the most relevant actions in the design of concrete structures [1]. It is particularly critical in reinforced concrete structures without shear reinforcement. In the Netherlands, there are several concrete slab bridges reinforced with plain bars and without shear reinforcement, these bridges were built before 1976 and by now are reaching the end of their service life [2]. The shear capacity of these structures is of concern and the development of a proof load test to evaluate their safety is necessary.

Proof load testing is the application of a predetermined load on a structure, where a response is measured and compared with a predefined stop criterion that is based on measured structural responses such as the strain of the reinforcement, the crack width, and deflection. Stop criteria for proof loading tests for bending moment failures are available in codes and guidelines [3] [4], however, none of them can be used for shear failure tests.

To overcome this, experiments were carried out in the Stevin lab at TU Delft [5] to develop a stop criterion that can be included in the future Dutch guidelines for proof load testing. The measurements from these experiments are used as base for the development of this project.

Yang [6] proposed that the opening of the critical inclined crack can be considered as the lower bound for the shear capacity. This theory states that the critical shear displacement of an existing flexural crack can be used as the criterion for the opening of the critical inclined crack.

In this project, measurements of Digital Image Correlation (DIC) were employed to obtain a refined measurement of the cracks kinematics, this method compares a reference image in an un-deformed state to a series of deformed images. DIC has an advantage over traditional measurement techniques because it allows tracking the evolution of the cracks even an instant before the failure.

The aim of this additional graduation work is to determine the crack kinematics of four beam tests (slab strips) by performing a DIC analysis and then to implement the proposed failure criteria [6]. Elizabeth Jones developed a Matlab-based DIC code that was later edited and improved by Ulric Celada (Ph.D. student) and in order to extract the shear displacements and the crack widths the author of this project performed adjustments and further improvements to some functions within Celada's code. With this information, the critical shear displacement can be related to the lower bound of the failure load and that can finally be linked to the crack width of an existing flexural crack, which can be monitored during a proof load test. Furthermore, a user manual of the complete DIC code was developed as part of this project.

### 1.2 OBJECTIVES

The aim of this project is to assess the crack kinematics of four beam experiments, using the Digital Image Correlation (DIC) technique in order to implement a stop criterion for shear failure based on the critical shear displacement.

The objectives are depicted as follows:

- 1. Compare the results obtained from the LVDTs measurements with the ones obtained using the DIC analysis in terms of horizontal displacement at the reinforcement level.
- 2. Use the DIC results to track the evolution of the cracks and classify them in major or secondary cracks.
- 3. Based on the shear displacement results, identify the critical cracks and the initiation of the collapsing process by finding the critical shear displacement.
- 4. Identify the lower bound of the failure load and link it to the crack width of an existing flexural crack.

# LITERATURE REVIEW

### 2.1 CRITICAL SHEAR DISPLACEMENT THEORY

### 2.1.1 INTRODUCTION

Yang [6] based on experimental observations, developed a new theory for the shear failure capacity of reinforced concrete members without shear reinforcement. This researched is based on the force transfer mechanisms that occur on a critical inclined crack or flexural shear crack as shown in Figure 2.1

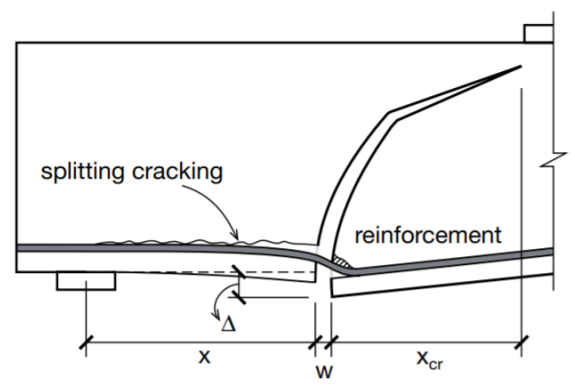


Figure 2.1 Free body of a flexural shear crack [9]

Yang [6] proposed that the shear displacement of the critical inclined crack can be considered as a failure criterion for the shear capacity of a structural member. The opening of the critical inclined crack is triggered when the shear displacement of an already formed flexural crack reaches a critical value.

A critical inclined crack is defined as the crack that originates from a flexural crack and then develops two secondary branches, one at the rebar level approaching the support and the other at the compression zone, see Figure 2.1. The name flexural shear crack is given to denote its origin.

Experimental observations show that the two ways in which reinforced concrete beams without shear reinforcement can fail due to a shear load, depend on whether the beams lose the bearing capacity or not, after the opening of a critical inclined crack.

The two failure modes are defined as:

- 1. Flexural shear failure, when the failure is caused by the opening of the critical inclined crack
- 2. Shear compression failure, when beams don't fail immediately after the opening of the critical inclined crack. In this case, the failure is caused by the crushing of concrete on the compression zone.

As it can be observed, the opening of the critical crack is an important aspect regarding the failure mode. It initiates with the opening of a secondary crack (dowel crack) which starts as a flexural crack and then develops along the tensile reinforcement. According to Yang [6], the opening of this dowel crack is conceived as the cause of the opening of the critical inclined crack. The development of this crack produces the detachment of the tensile reinforcement causing a decreased of stiffness in the tensile zone, increasing the crack width. With a larger crack width, a larger shear displacement is needed to reach the same shear stress level. This larger shear displacement produces more detachment of the reinforcement. The continuity of this process finally causes the collapsing of the beam.

It is important to note that not all flexural cracks are able to develop further to the compression zone of the beam, the cracks that are able to do it are denoted as major cracks. Such cracks are the only ones that can develop into the critical shear cracks.

The shear displacement of a flexural crack is influenced by the shear force, the bending moment and the profile of the crack at the cracked cross-section. The profile of a flexural crack is determined by the ratio between the moment and the shear force M/Vd. For small M/Vd ratios, the flexural cracks that develop are usually more inclined and have larger shear displacements, which means that these cracked sections have lower shear resistance. However, a large sectional moment is needed to allow the formation of flexural cracks. On the other hand, cracks that form in sections with larger M/Vd ratios are perpendicular to the longitudinal direction of the beam and have similar crack profiles. In these sections, the crack width plays an important role, since larger crack widths are expected resulting in a lower shear resistance. Figure 2.2 is taken from [9], it shows the shear resistance of the cracked sections with respect to their location. In slender beams, cross sections with large M/Vd ratios become more dominant, thus Yang [6] modeled the opening of a crack at this location.

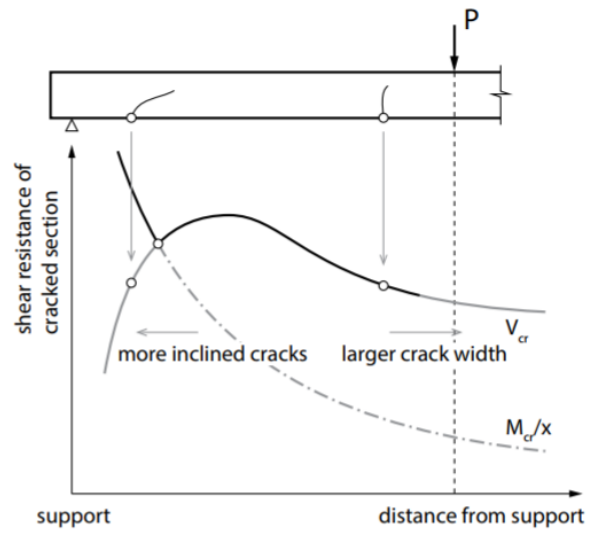


Figure 2.2 Cracked sections with respect to their location [9]

The shear force level at which the first critical inclined crack develops is denoted as the inclined cracking load  $V_{cr}$ . Therefore, the inclined cracking load  $V_{cr}$  is suggested as an indicative measure of the shear capacity of a structural member and can be considered as a lower bound of  $V_u$ .

Yang [6] proposed a criterion to quantify the shear displacement  $\Delta$  at the level of the tensile reinforcement. This  $\Delta$  indicates the shear displacement of the crack and is

related to the shear stress generated by aggregate interlock when the crack width is known.

The critical shear displacement  $\Delta_{cr}$  is defined as the shear displacement at which the collapsing process will start. It is assumed to be a constant value in all the crack sections of a given beam. Once  $\Delta$  is higher than  $\Delta_{cr}$  the crack will develop into a critical inclined crack.

# 2.2 MODEL-BASED ON A CRITICAL SHEAR DISPLACEMENT

Yang [6] developed a new model based on the critical shear displacement. This model was simplified enough to be used in practice. Some of these simplifications will be briefly described in the following subsections.

#### 2.2.1 SIMPLIFIED CRACK PATTERN

It has been generally accepted that if a free body diagram is taken from a beam along a flexural crack as shown in Figure 2.3, the shear force can be transferred by the following four mechanisms, summarized by ACI-ASCE Committee 445 on Shear and Torsion:

- 1. Shear stress in the uncracked concrete zone
- 2. Aggregate interlock caused by the tangential displacement of the crack faces
- 3. Residual tensile stress occurring at limited normal opening of the cracks
- 4. Dowel action caused by the longitudinal bars

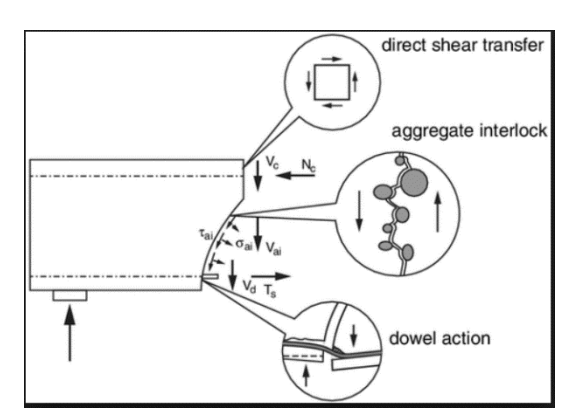
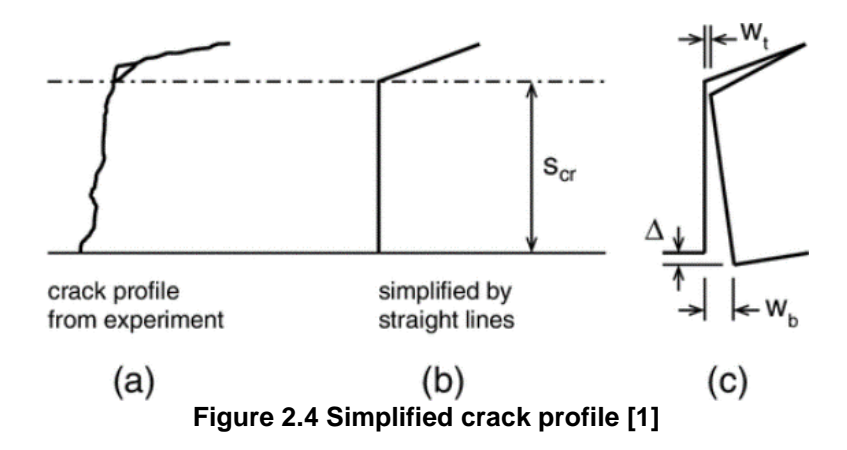


Figure 2.3 Free body diagram with shear transfer mechanism [1]

Regarding aggregate interlock, the aspects that contribute the most to the shear force transmission are the crack shape and the normal and tangential displacements along the crack profile. The crack profile is characterized by the shape of the crack path and the distribution of the crack openings along the crack.

To arrive at the simplified crack pattern some assumptions must be made. From Yang [10] Figure 2.4 shows a flexural crack generated at a cross section with large *M/Vd* and two important assumptions are made:

- 1. The crack is composed of two branches: the major crack or main branch and the secondary branch located in the compressive zone. The latter allows additional shear displacement in the major crack part when the shear force increases
- 2. The major crack can be simplified as perpendicular to the longitudinal direction of the beam.



In the main branch of the crack, the shear displacement generates aggregate interlock stresses while the secondary branch allows the shear displacement in the major crack. This simplification allows the normal crack opening and the shear displacement of the major crack to be independent.

The distribution of the crack opening varies linearly, and the shear displacement becomes constant. The crack width at the top of the main branch  $w_t$  depends on the inclination and the opening of the secondary branch, the value is assumed to be constant.  $w_t$ =0.01 mm. While the crack width at the reinforcement level is estimated considering the crack spacing and the steel stress with the following equation:

$$W_b = l_{cr,m} \mathcal{E}_s \tag{1}$$

If the height of the fully develops crack is  $S_{cr}$ , the space between a fully develop crack and the next possible cracked section is:

$$l_{cr,m} = \frac{s_{cr}}{k_c} \tag{2}$$

It is assumed that for a major crack, its total height is reached directly after its formation and determined by cross-sectional equilibrium. The height can be determined by:

$$s_{cr} = \left[1 + \rho_s n_e - \sqrt{2\rho_s n_e + (\rho_s n_e)^2}\right] d$$
 (3)

# 2.2.2 SIMPLIFIED SHEAR FORCE-DISPLACEMENT RELATIONSHIP

Applying the assumptions developed for the simplified crack profile, the shear force transfer by aggregate interlock ( $V_{ai}$ ) can be determined by relating the shear stresses and the displacements at the cracked faces.

Adopting the analytical shear stress expression proposed by Walraven [11]:

$$\tau_{ai} = \sigma_{pu} \left\{ \mu A_X [\Delta, w(s)] + A_y [\Delta, w(s)] \right\}$$
 (4)

The total shear force transferred along the crack can be expressed as:

$$V_{ai} = \int_{0}^{S_{cr}} \tau_{ai}[\Delta, w(s)]bds = \sigma_{pu}b\int_{0}^{S_{cr}} \mu A_X(\Delta, w) + A_y(\Delta, w)ds$$
 (5)

However, this is a complex equation, so considering the simplification of the crack profile, the application of Walraven's aggregate interlock expression becomes possible, substituting  $\sigma_{pu}=6.39\,f_c^{0.56}$  in Eq. (5) becomes [1]:

$$V_{ai} = 6.39 f_c^{0.56} b s_{cr} v_{ai}$$
 (6)

with

$$\upsilon_{ai} = \int_{w}^{w_b} [\mu A_x(\Delta, w) + A_y(\Delta, w)] dw$$
 (7)

Where  $A_x$  and  $A_y$  refer to the projected areas of the cracked surface of a unit crack length according to Walraven, being functions of the tangential and normal displacement  $(\Delta, w)$  of the two cracked faces.

$$V_{ai} = 6.39 f_c^{0.56} b \frac{0.003}{w_b - 0.01} (-978\Delta^2 + 85\Delta - 0.27)$$
 (8)

## 2.3 CRITICAL SHEAR DISPLACEMENT

The total shear force transmitted across the cracked section is determined by the summation of the three transfer components:

$$V = V_c + V_d + V_{qi}$$
 (9)

Where the force transferred in the compression zone is denoted by  $V_c$  and determined with Mörsch's approach [12], where a linear stress distribution in the compression zone is assumed and the residual stresses in the crack are neglected:

$$V_c = \frac{2}{3} \frac{z_c}{z} V = \frac{d - s_{cr}}{d + 0.5 s_{cr}} V$$
 (10)

The shear force transferred by dowel action is denoted by  $V_d$ . It is calculated using the expression proposed by Bauman and Rüsch [13]:

$$V_d = 1.64 b_n \phi_3^3 \sqrt{f_c}$$
 (11)

It is assumed that the maximum dowel force occurs when  $\Delta_{cr}$  is reached [6]

The force transferred by aggregate interlock can be determined with Eq. 6 or the simplified version Eq. 8. However, to calculate  $V_{ai}$ , the crack width at the level of the tensile reinforcement  $w_b$  and the critical shear displacement  $\Delta_{cr}$  must be determined. The crack width is based on the bending moment in the cross-section:

$$w_b = \frac{M}{zA_aE_a}l_{cr,m} \tag{12}$$

Now the only unknown is the critical shear displacement  $\Delta_{cr}$ . However, the determination of  $\Delta_{cr}$  is difficult since it is not possible to predict the exact position of the critical crack and the crack profile.

To solve this unknown Yang [6] carried out a back analysis based on the shear test results from existing databases, more information can be found on the reference document. With the results, a plot of the  $\Delta_{cr}$  against the depth of the beams was constructed, as shown in Figure 2.5 Calculated critical shear displacement against effective height .

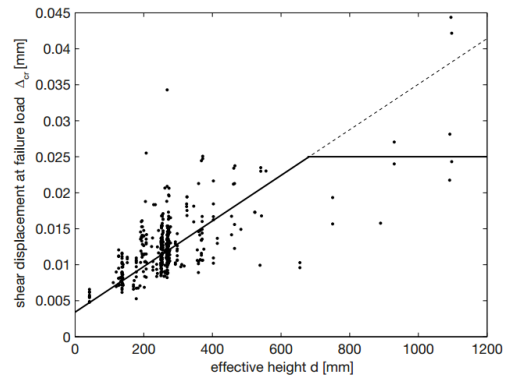


Figure 2.5 Calculated critical shear displacement against effective height [6]

From these results, it can be observed that the values of  $\Delta_{cr}$  fall in a range in between 0.005 and 0.05 mm presenting a relatively large scatter. Yang [6] suggested an expression for  $\Delta_{cr}$  based on a regression analysis:

$$\Delta_{cr} = \frac{d}{29800} + 0.005 \le 0.025 mm \tag{13}$$

Yang [6] proposed that the rebar diameter has an influence on  $\Delta_{cr.}$  For instance, under the same dowel force, a larger rebar diameter will display a lower dowel displacement due to the higher flexural stiffness. Meaning that a smaller shear

displacement might develop the same crack when the rebar diameter is larger. Eq. 13 was adjusted to consider the diameter of the tensile bar:

$$\Delta_{cr} = \frac{25d}{30610\phi} + 0.0022 \le 0.025mm \tag{14}$$

# 2.4 EVALUATION OF THE SHEAR CAPACITY BASED ON THE CRITICAL SHEAR DISPLACEMENT

The following flow chart (Figure 2.6) resumes the steps that must be followed to determine the shear capacity of a slender reinforced concrete beam without shear reinforcement considering the critical shear displacements:

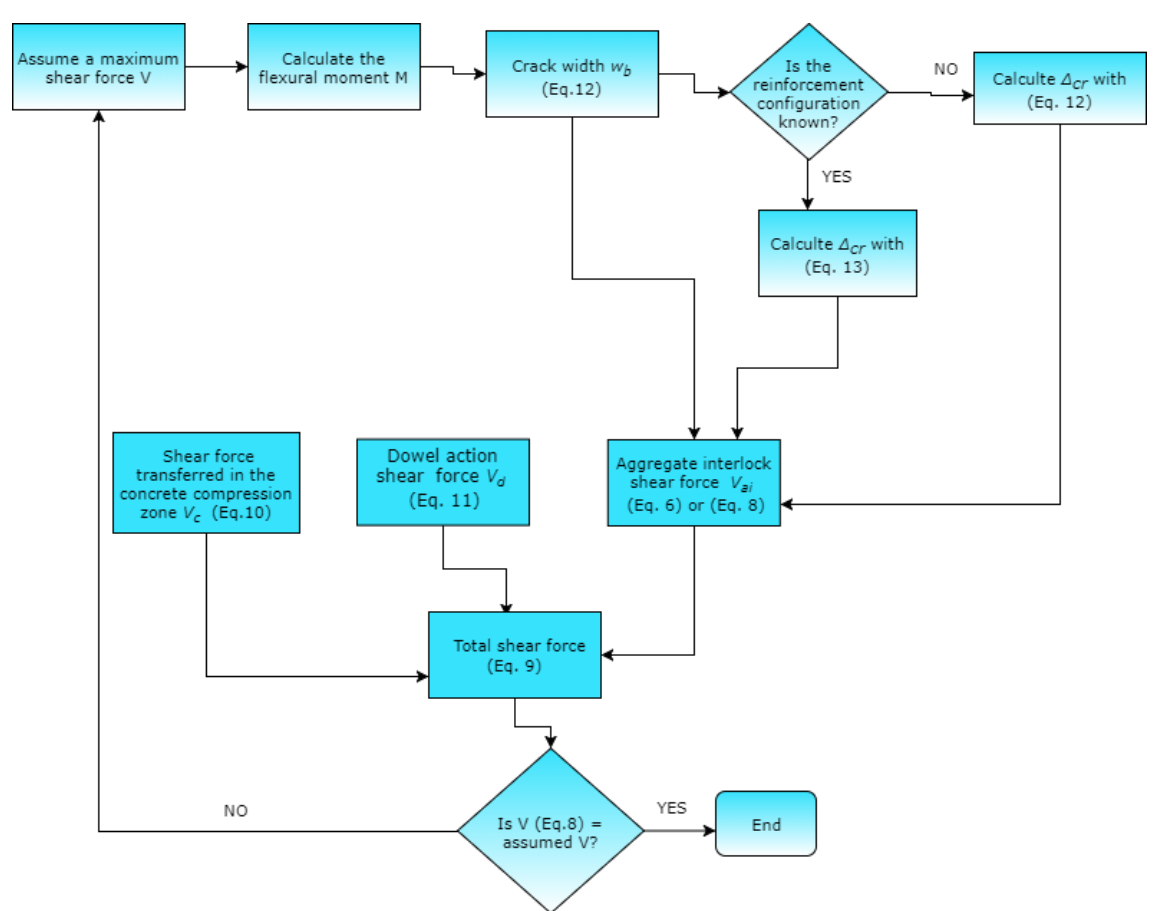


Figure 2.6 Flow chart of the evaluation of the shear capacity based on critical shear displacement

# 2.5 CRACK WIDTH LIMIT ON AGGREGATE INTERLOCK

A stop criterion should be based on a measurable quantity. Since during proof load tests, the common measured responses are the strains, deformations and crack widths, the most suitable response to be linked to a stop criterion based on the theory of critical shear displacement is the crack width.

The shear transfer mechanism that is related to the shear displacement in cracked faces is the aggregate interlock. This mechanism is activated with the transfer of stresses produced by the tangential displacement of the cracked faces because of the protruding aggregates. Therefore, the stop criterion should be based on a cross-section that is already cracked in bending.

Yang [6] derived an improved formulation to calculate the shear force transfer by aggregate interlock, see Equation (8). This formulation was based on the simplification of the crack profile, which allowed to detach the dependency of the shear displacement and the crack width. The crack opening along the crack profile was assumed to vary linearly with a crack width at the top of  $w_{\ell}=0.01$  mm to the crack width  $w_b$  at the bottom of the cross-section.  $w_b$  can be calculated using Equation (12).

To develop a stop criterion based on the expression of aggregate interlock, the stop criterion should be expressed as a function of  $w_b$ , which can be measured during the test. [14] The formulation can be expressed as:

$$w_b = \frac{0.03 f_c^{0.56} s_{cr} b (978 \Delta_{cr}^{-2} + 85 \Delta_{cr} - 0.27)}{V_{oi}} + 0.01$$
 (15)

Considering that the critical shear displacement  $\Delta_{cr}$  is identified as the shear displacement at which the collapsing process starts,  $w_b$  could be used a stop criterion. This criterion is most suitable for sections where the critical inclined crack develops from an existing bending crack since the crack will develop more gradually and can be better monitored during a proof load test.

# EXPERIMENTAL PROCEDURE

In this section, a summary of the properties of the specimens and the test set up is presented. This project is based on the experimental results of four beams selected from the series of beam tests that studied the influence of the reinforcement type (ribbed or plain) and the height of the specimen [2].

### 3.1 SPECIMENS AND TEST SET UP

In total, four beam experiments were studied:

- 1. P502A2 tested in bending
- 2. P804B1 that was not previously cracked and fails in shear
- 3. P804A1 first tested in bending and,
- 4. Then tested until it fails in shear P804A2

These beam experiments were previously analyzed by Lantsoght [7]. The beams were labeled with an identifying code. The first letter corresponds to the rebar type (P: plain rebar), the following two numbers referred to the beam height (h=300mm or 800 mm), the next number refers to the number of the specimen, the subsequent letter to the end of the specimen and the final number to the loading position.

The details of the beams properties and failures modes are summarized in Table 1. The details of the reinforcement configuration are shown in Figure 3.1.

**Table 1 Beams Properties** 

Beam	Reinforcement (Plain bar)	Reinforcement ratio [%]	h (mm)	b [mm]	a [mm]	a/d	Concrete cube strength [MPa]	Peak load [kN]	Failure mode
P502A2	3 Ø 20	0.68	500	300	1000	2.15	87.2	148.8	Flexural
P804B1	6 Ø 20	0.84	800	300	2500	3.31	85.1	185.6	Shear
P804A1	6 Ø 20	0.84	800	300	3000	3.97	85.1	207.4	Flexural
P804A2	6 Ø 20	0.84	800	300	2500	3.31	85.1	231.7	Shear

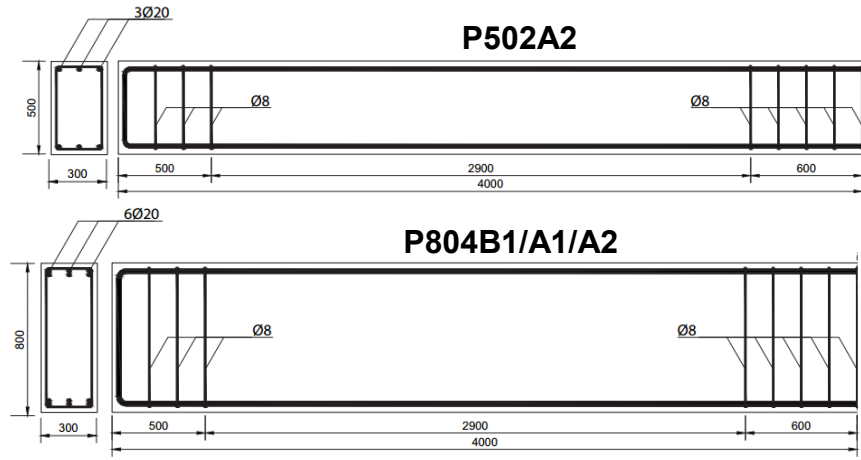


Figure 3.1 Reinforcement Layout. [5]

The specimens were simply supported and loaded by a point load. The position of the load changed between the tests to accomplish the expected failure. Figure 3.2 shows the position of the supports and the application of the load for the studied beams.

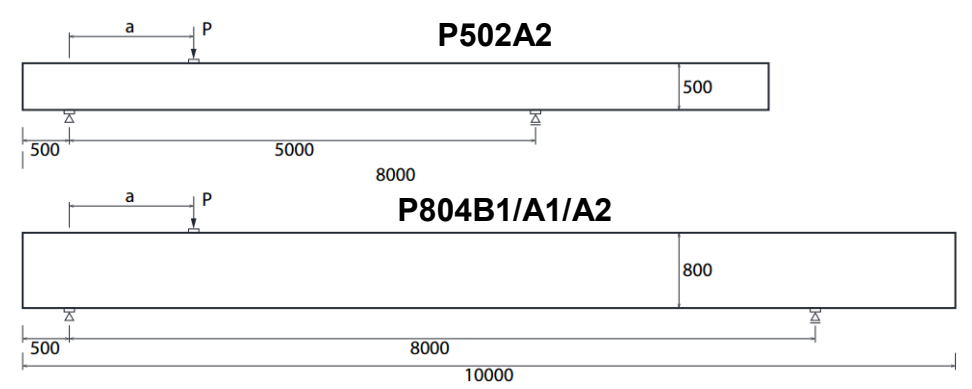


Figure 3.2 Configuration of the tests. [5]

In all the test, several measurements were performed, for the complete information refer to [5]. For this research the relevant measurements are the ones related to the crack openings and the load levels, which were obtained in the following way:

- The force was measured with the load cell,
- For the crack openings, an LVDTs array was placed. It consisted of horizontal LVDT's located at the tensile reinforcement level and at the mid-height of the specimens. This research focuses on the values obtained at the reinforcement level.



Figure 3.3 Typical LVDT's array

### 3.2 DIGITAL IMAGE CORRELATION MEASUREMENTS

In addition to the conventional LVDTs, the use of Digital Image Correlation (DIC) measurement was implemented. The main advantage of the DIC technique is that it can perform a full-field measurement of the displacements associated with the opening of the cracks. For this purpose, images are recorded during the entire experiment and post-processed to find displacements and strains. For these experiments, the pictures were taken with a camera of 5616 by 3744 pixels resolution and the data was post-processed using the Matlab-based DIC code programmed by Elizabeth Jones [8] and improved by Ulric Celada (visiting Ph.D. student).

The Digital Image correlation technique is a digital measurement method that provides measurements of an entire specimen surface by comparing a reference image in an un-deformed state to a series of deformed images. The basic principle consists in dividing the reference image into square subsets of pixels (e.g. 21 x 21 pixels), which have a unique pattern and tracking this points or patterns between the recorded images. Once the location of this subset is found in the deformed image, the displacements can be determined in terms of pixels.

To implement the DIC technique, a pattern was painted on the surface of the specimens as shown in Figure 3.4.



Figure 3.4 Typical DIC painted pattern

# RESULTS AND DISCUSSION

In this section, the results for the studied beams are presented. First, a description of the procedure followed for obtaining the results is given, the results for test P804B1 are shown. Finally, a summary of the results of all the beams and the discussion are presented.

### 4.3 GENERAL APPROACH

The development of this project involved several steps, the main aspects are shown in the following figure:



First, the data was correlated and post-processed using the Matlab-based DIC code programmed by Elizabeth Jones [14] and improved by Ulric Celada (visiting Ph.D. student).

The procedure followed to run a typical correlation for the DIC is summarized in Figure 4.2. For detailed information consult the manual in Appendix A.

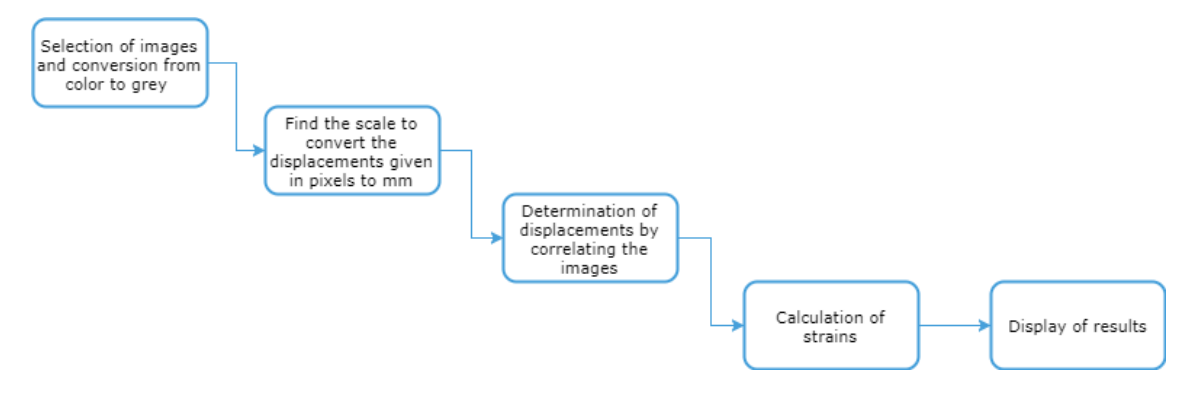


Figure 4.2 Steps for a typical correlation using the Matlab-based DIC code

The general procedure started with the selection of the images to be correlated and the conversion from color to grey scale. Approximately 3 pictures were chosen at every representative load level, the pictures were taken with a difference of two seconds between each one. The final pictures were taken approximately one or two seconds before failure.

Then, the proper scale to convert the displacements given in pixels to millimeters (mm) was found, for this purpose a template with 9 red points was set near the beams

during the experiment. The distance between the red points was known (80 mm), therefore a relation between the pixels and mm could be found.

The determination of the displacements consisted in correlating the images. First, the reduced images were correlated using a large subset size and sparse grid and then the full-sized images were correlated using a denser grid. Finally, the strains were calculated using a 4-noded linear element. The results were displayed using the equivalent strains.

To obtain the information of the crack kinematics, a Matlab script from Ulric Celada was adapted to obtain horizontal and vertical displacements at selected points. This script allows using an image, usually, the results from the last correlated image, as background to select the correct pair of points or coordinates to get the displacements. This script was first used to validate the results found from the DIC analysis by comparing the measurements of the horizontal displacements of the LVDTs at the reinforcement level and the displacements found from the post-processing of the DIC data. Then, it was implemented to obtain the cracks kinematics by selecting a point to the left and right side of each crack at the reinforcement level. Figure 4.3 shows a flow chart of the procedure followed to find the cracks kinematics.

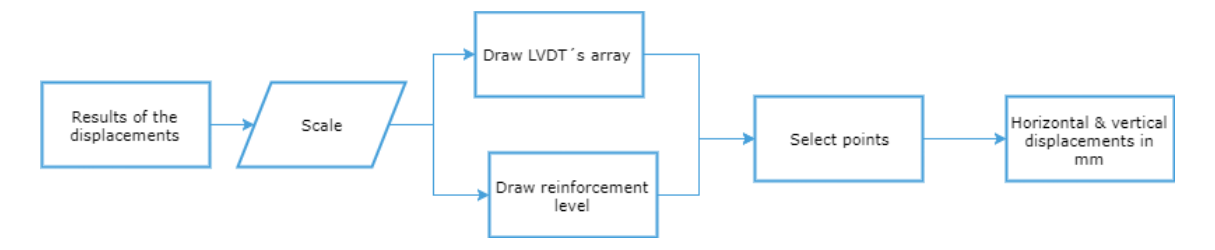


Figure 4.3 Procedure to obtain vertical and horizontal displacements

Table 2 shows a summary of the total number of images used, the loading cycles and levels, as well as the final subset and grid size and the scale used for the DIC analysis.

**Table 2 DIC parameters** 

Test	Failure mode	Load cycles	Load levels	Number of images	Subset size (pixels)	Grid size (pixels)	Scale (mm/pixel)
P804B1	Shear	0	11	48	71	30	0.4260
P502A2	Flexural	3	9	34	71	30	0.3472
P804A1*	Flexural	42	8	68	121/91	30	0.4570/0.4541
P804A2	Shear	17	5	29	91	30	0.4447

<sup>\*</sup>Test P804A1 was divided into two parts since the position of the camera changed during the test.

The final step was to analyze the results. Figure 4.4 shows a summary of the procedure. The results of all the beams were obtained following the same methodology.

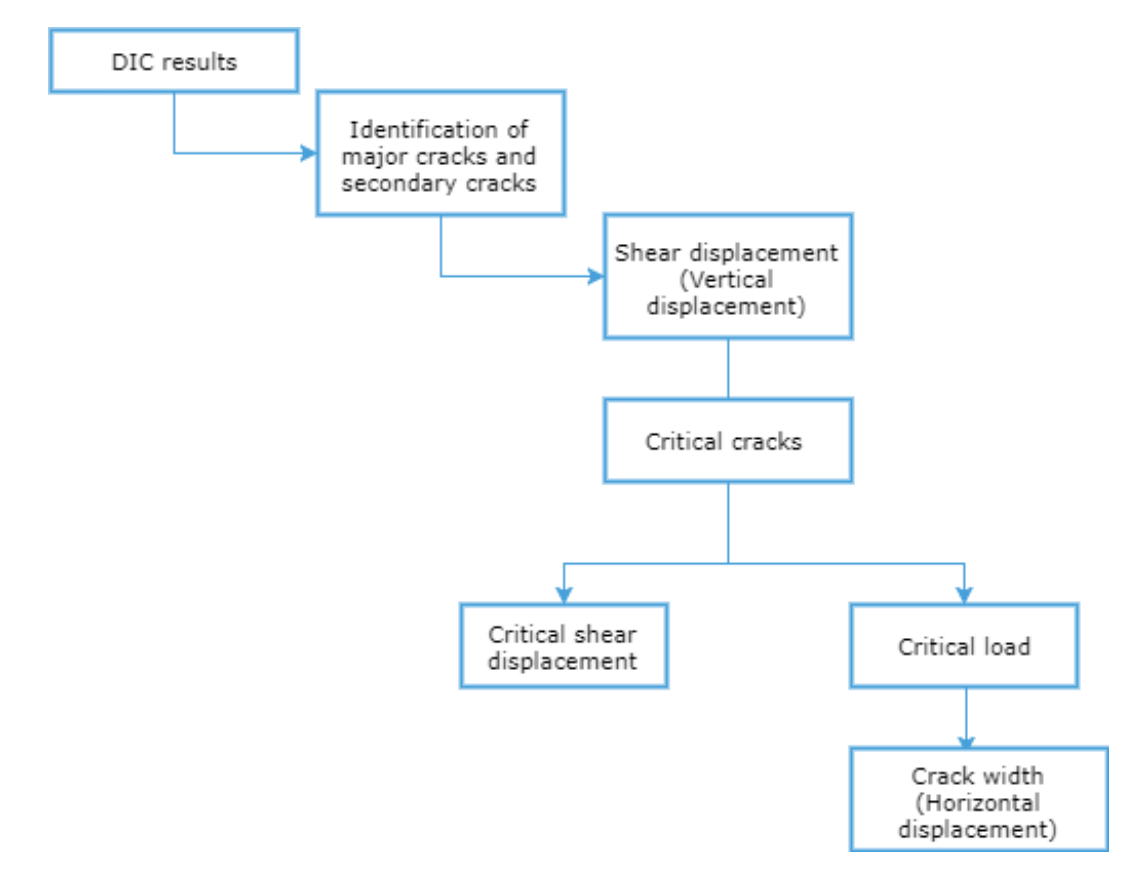


Figure 4.4 Procedure to obtain the critical shear displacement, critical load and crack width

## 4.4 DESCRIPTION OF RESULTS

In this research, the measurements of interest are the load, the crack profile and the information regarding the crack width and the shear displacements. The results were obtained in the following way.

First, the loading scheme measured during the test was compared with the ones obtained from the pictures used for the digital image correlation. Figure 4.5 shows the loading scheme measured during the experiment and the one obtained from the pictures used for the digital image correlation for P804B1.

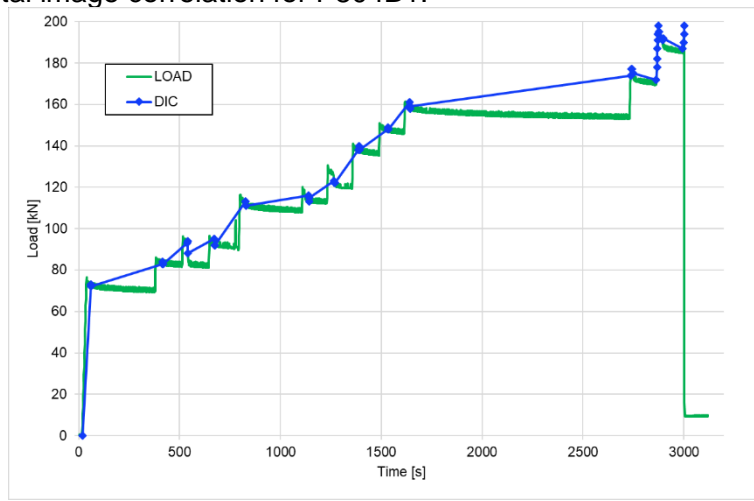
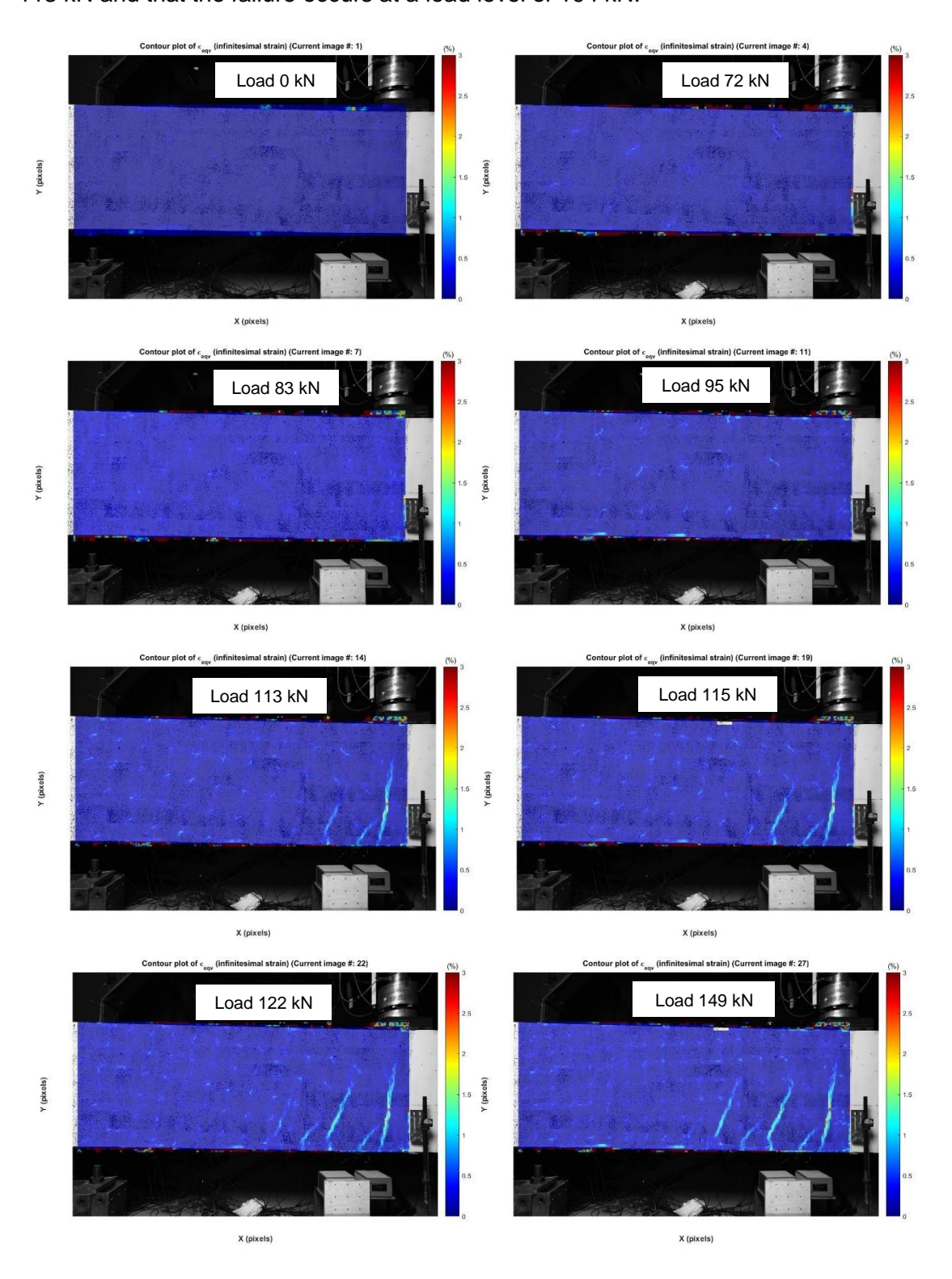
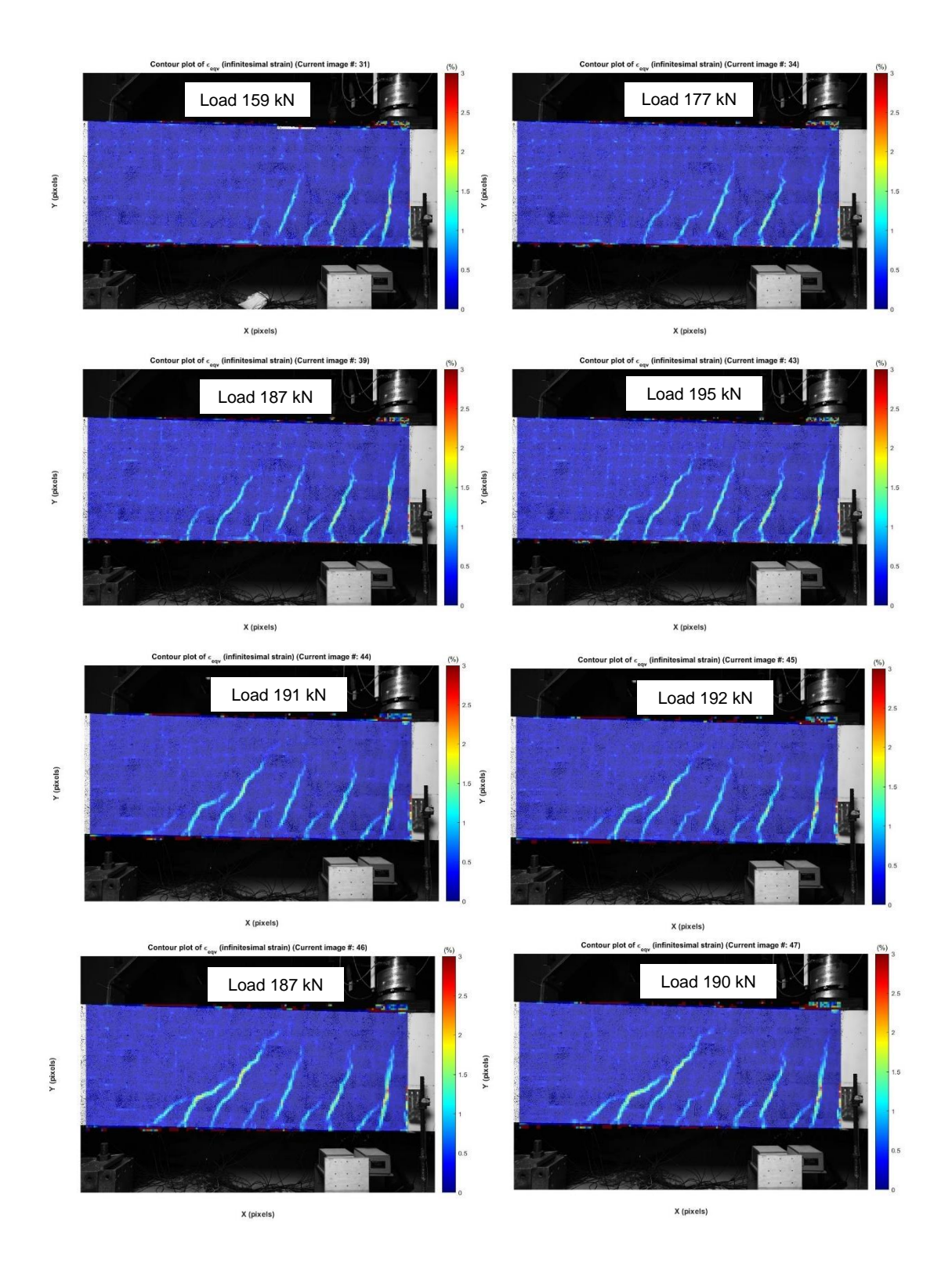


Figure 4.5 Loading scheme for P804B1

Then, the results of the DIC analysis were shown at the representative load levels, the equivalent strains were chosen for display. In Figure 4.6, the results for the representative load steps are shown for P804B1. The pictures clearly show the evolution of the profile of the cracks. It can be observed that the first cracks are visible at a load of 113 kN and that the failure occurs at a load level of 194 kN.





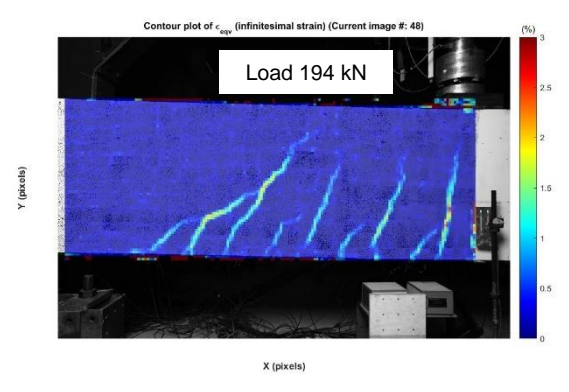


Figure 4.6 DIC results for representative load levels for P804B1

Second, as mention in the previous section, a comparison was made between the measurements of the horizontal displacements of the LVDTs at the reinforcement level and the displacements found from the DIC measurements. In Figure 4.7, the LVDTs location is shown, as well as the drawn array used for the comparison.

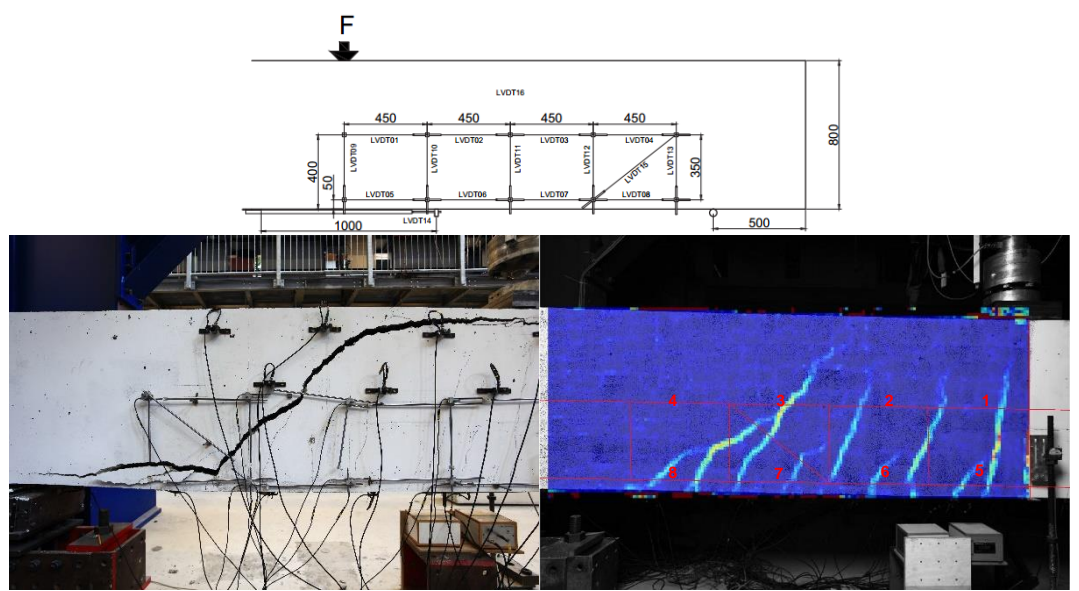


Figure 4.7 LVDTs array location for P04B1

Figure 4.8 shows the comparison of the results for P804B1. In the plots, the values of the horizontal displacement are plotted against the time of the experiment. The results of horizontal displacements show a relatively high scatter and differ significantly from the LVDTs measurement, especially when the LVDTs values are below 0.1 mm.

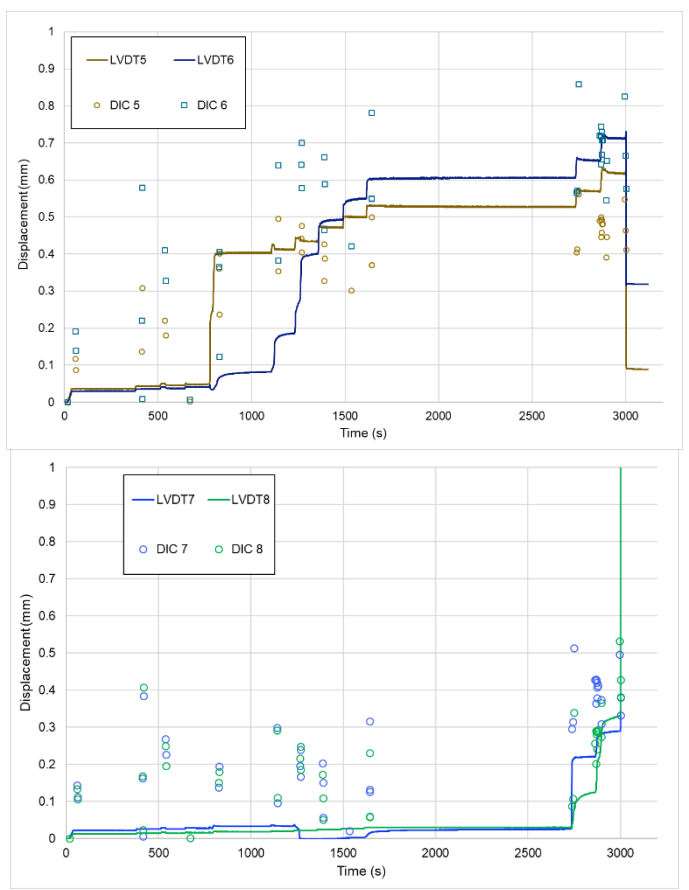


Figure 4.8 Comparative of the horizontal deformation development of LVDT's 5-8 & DIC (bottom row) for P804B1

Finally, the results obtained from the DIC analysis for each crack were obtained in terms of shear displacement (vertical displacement) and crack width (horizontal displacement) at the tensile reinforcement level. For that purpose, the reinforcement level was drawn to help with the selection of the points as it can be observed in Figure 4.9 for beam P804B1. This figure also shows the identification of the cracks, which facilitated the classification of the cracks in major or secondary cracks. Four major cracks (1, 3, 5 & 7) and five secondary cracks (2, 4, 6, 8 & 9) were identified.

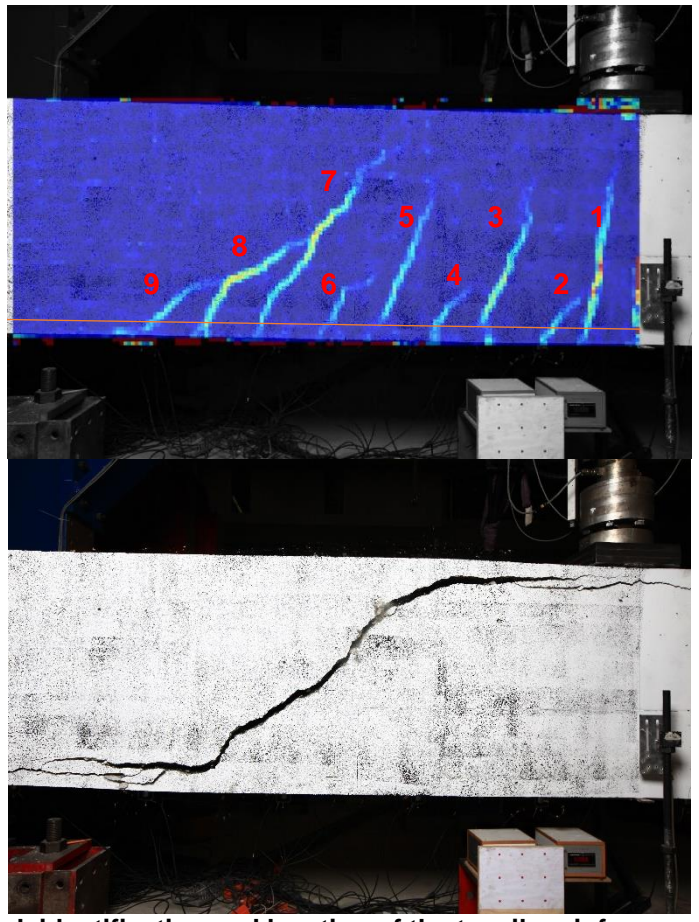


Figure 4.9 Crack identification and location of the tensile reinforcement for P804B1

The results for shear displacement are presented in a plot constructed with the values of shear displacement against the measured load. These values are the result of the averaging of 3 vertical displacements. Figure 4.10 shows the results for the major cracks and Figure 4.11, for the secondary cracks.

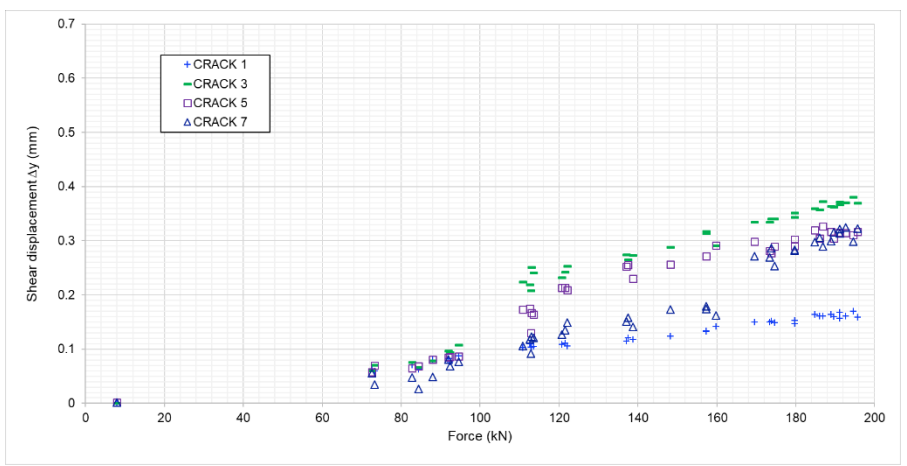


Figure 4.10 Shear displacement for major cracks for P804B1

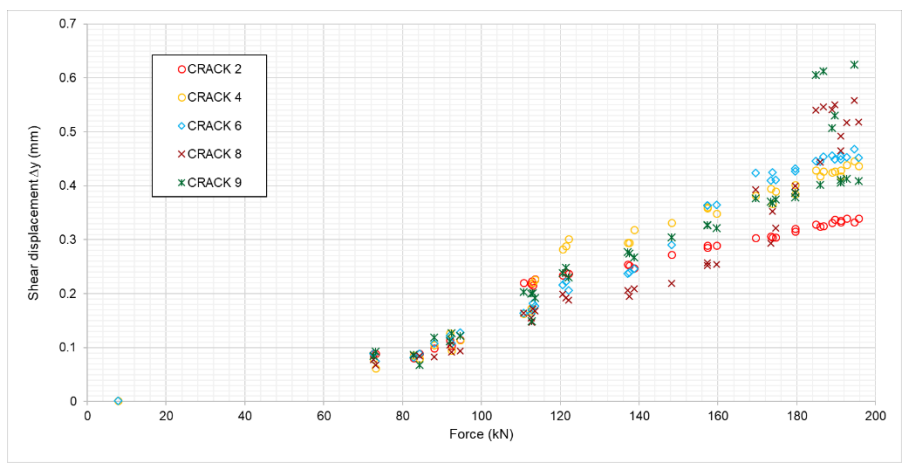


Figure 4.11 Shear displacement for secondary cracks for P804B1

After analyzing these results, it was concluded that cracks 8 and 9 are the critical cracks. For example, in Figure 4.12, it can be observed that from the load step of 180 kN and onwards the behavior is different from the previous load steps. The red continuous line represents the load level from which the shear displacement triggers, it is equal to the 92% of the collapse load. At this load level, the shear displacement could be identified as the critical shear displacement. The value is equal to 0.40 mm.

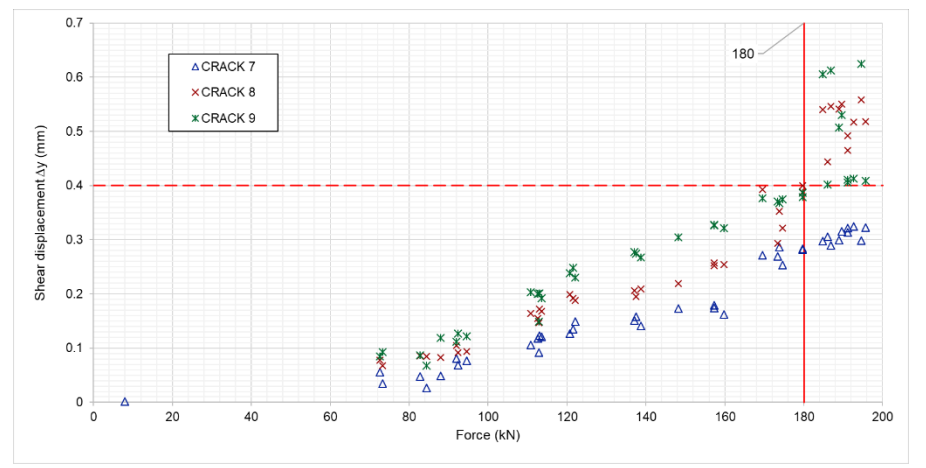


Figure 4.12 Critical inclined cracks and critical shear displacement for P804B1

Finally, the values of crack width were plotted against the measured load. Figure 4.13 presents the results for the major cracks and Figure 4.14 for the secondary cracks. Cracks7, 8 and 9 present a more unstable behavior.

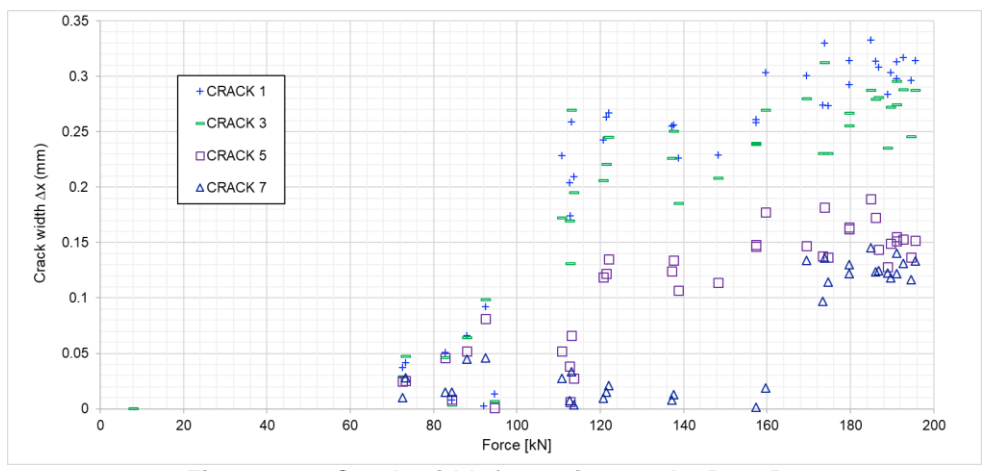


Figure 4.13 Crack width for major cracks P804B1

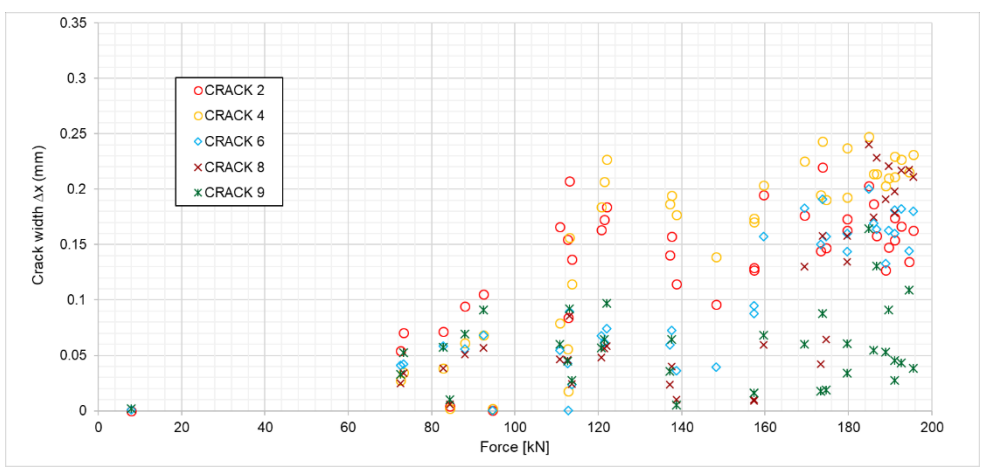


Figure 4.14 Crack width for secondary cracks P804B1

Once the critical load level was identified as 180 kN, the crack width found at this load level was of 0.31 mm. Thinking of a possible proof load test, Crack 1 was chosen since it is the first crack that appears and it is more probable that it could be instrumented.

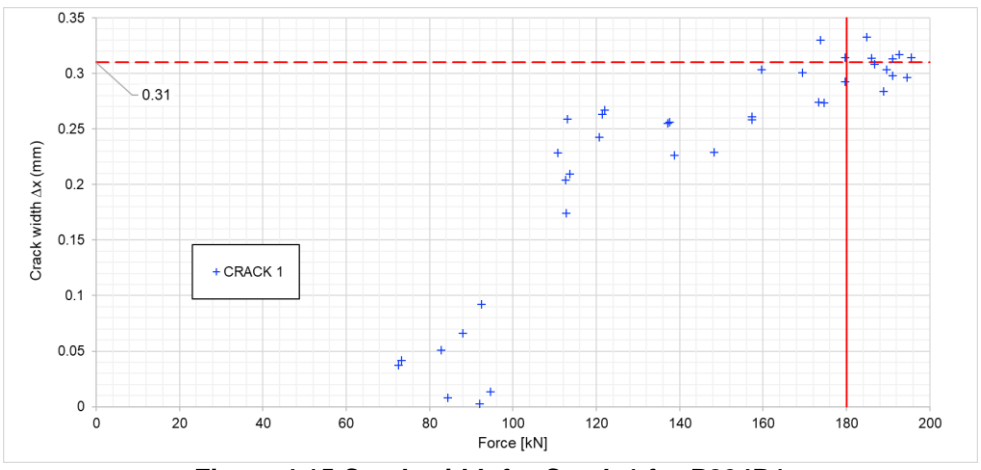
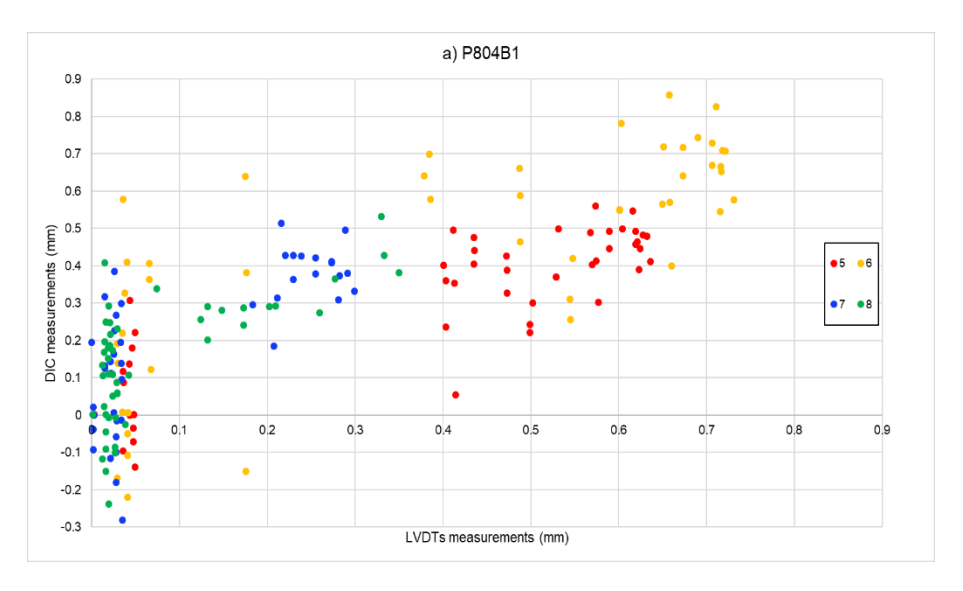


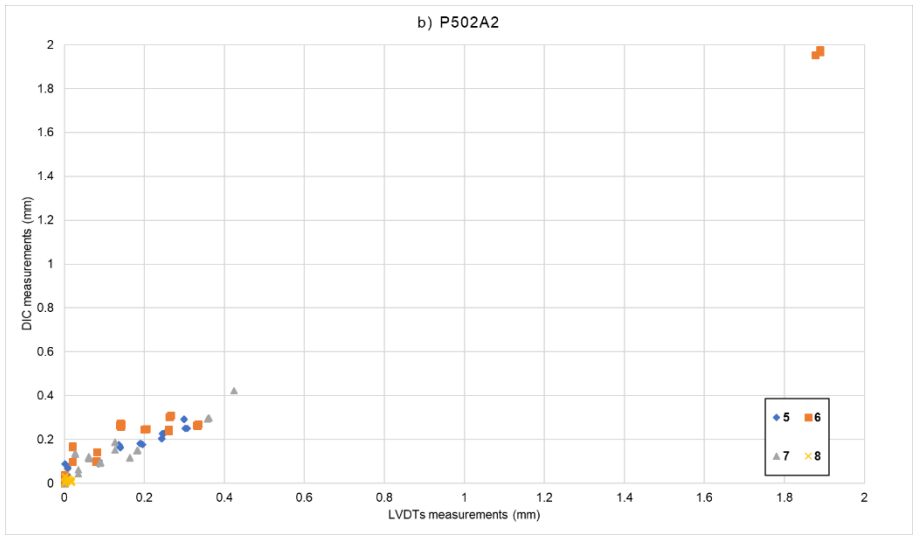
Figure 4.15 Crack width for Crack 1 for P804B1

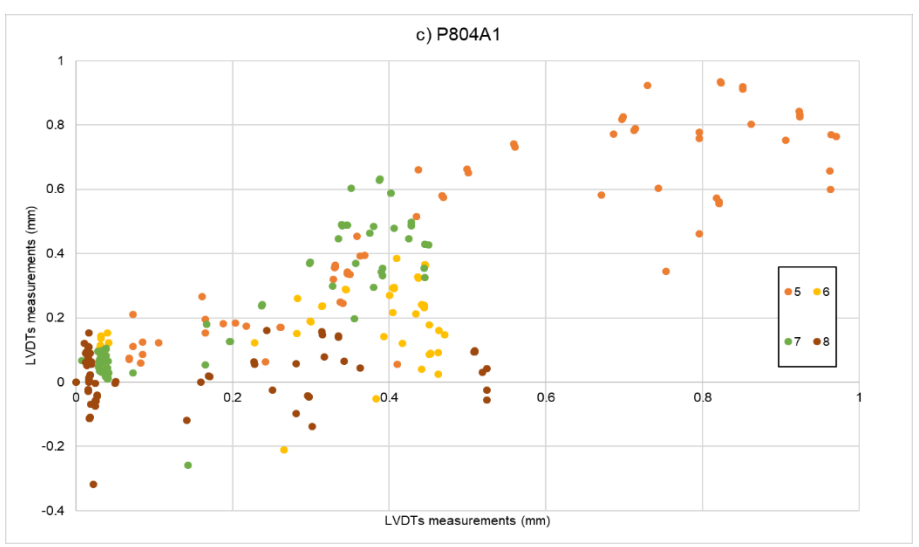
The remaining results of the tests can be found in Appendix B.

# 4.5 DISCUSSION

Figure 4.16 shows the graphs of the LVDTs against the DIC measurements.







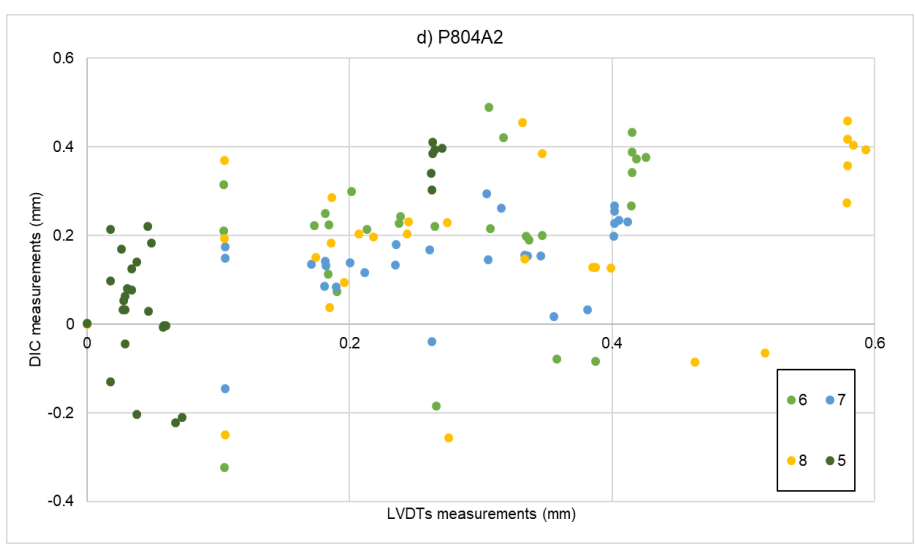


Figure 4.16 LVDTs vs DIC measurements for all test

Table 3 shows a summary of the identification of major and secondary cracks as well as the critical cracks found in the four tests. Figure 4.17 shows the cracks identification for each test.

Table 3 Crack identification for all beams

Table 6 Grack Identification for all beams									
Test	Failure mode	Total number of Cracks	ID of major cracks	ID of secondary cracks	ID of Critical Cracks				
P804B1	Shear	9	1, 3, 5 & 7	2, 4, 6, 8, & 9	8 & 9				
P502A2	Flexural	4	1, 2, 3 & 4	0	3 & 4				
P804A1	Flexural	5	1,3 & 4	2 & 5	2 & 5				
P804A2	Shear	7	1, 2, 3 & 5	4, 6 & 7	4 & 7				

Table 4 shows a summary of the cracks kinematics results for all the beams.

**Table 4 Crack kinematics for all beams** 

Test	Failure mode	Failure load (kN)	ID of Critical Cracks	Critical Load (kN)	% of Failure Load	Deformation profiles criterion P <sub>lim</sub> (kN) *	Critical shear displacement ∆ <sub>cr</sub> (mm)	Crack width for Crack 1(mm)
P804B1	Shear	185.6	8 & 9	180	92	110	0.40	0.31
P502A2	Flexural	148.8	3 & 4	125	84	125	0.21	0.15
P804A1	Flexural	207.4	2 & 5	180	87	120	0.40	0.28
P804A2	Shear	231.7	4 & 7	200	86	200	0.50	0.20

\*Lantsoght [13] analyzed the same beam experiments and proposed a stop criterion based on the deformation profiles obtained from the measurements of the horizontal displacements of the LVDTs.

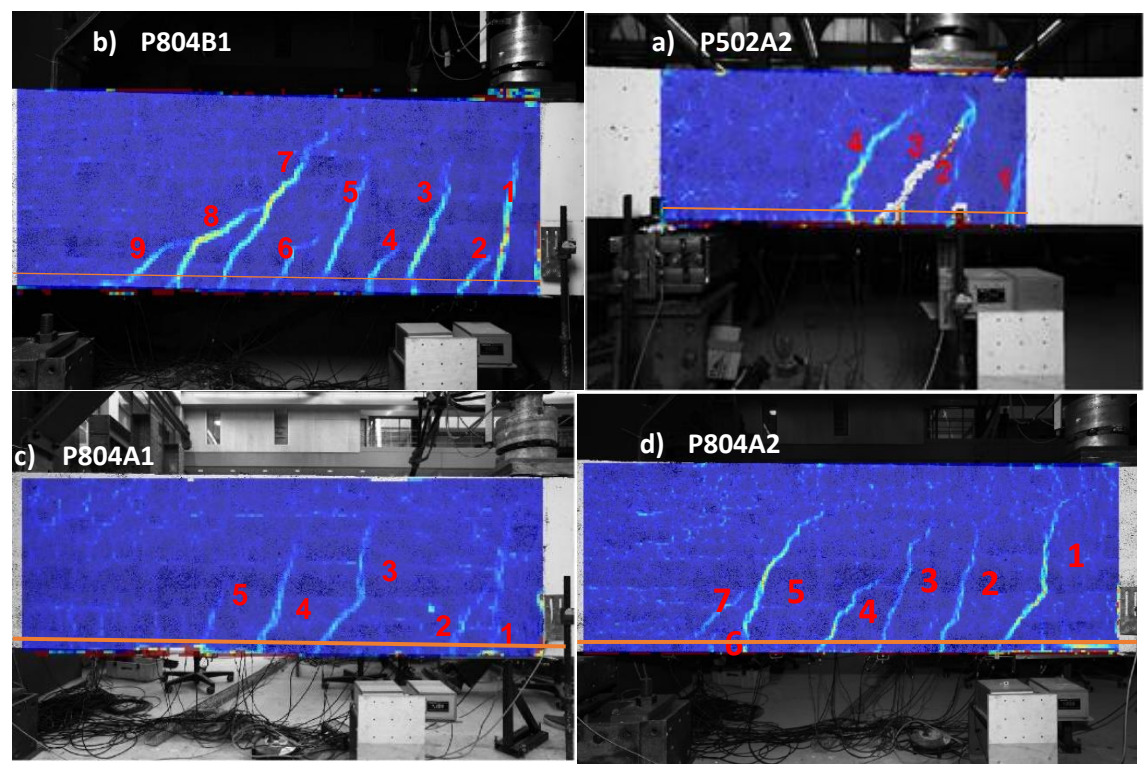


Figure 4.17 Crack identification

Figure 4.16 shows the graphs of the LVDTs against the DIC measurements of all the tests. These plots show how close the measurements are from each other. If the results were similar the points will arrange, and a straight line would be visible, which is the case for the test P502A2. Test P804B1, shows a high scatter, especially for the values of the LVDTs that are smaller than 0.1 mm. Test P804A1 and P804A2 show a high scatter and it is difficult to find a relation between the measurements, which means that the results cannot be compared and that different points are being measured. Some possible explanations for the difference in the results are that the location of the LVDTs array in the beam coincided with the location of some cracks, making it difficult to choose the corresponding coordinates for the DIC measurements and that the position of the camera changed during the experiments, which hindered the correlation process reflected in the results of the test P804A1 and P804A2.

The DIC results allowed to clearly observe the evolution of the profile of the cracks even a second before failure. For test P804A1, the images did not correlate well which can be observed in the DIC results. The main reason is that the pattern was not applied uniformly and portions in the right part of the painted surface in the beam were missing, therefore the algorithm was not able to correlate accurately those points.

The cracks were divided into major and secondary cracks. The major cracks are the ones that develop up to the compression zone and the secondary cracks are the ones that stayed at the reinforcement level.

Regarding the cracks kinematics, the shear displacement increased as the load level increased, following an almost linear behavior until a load where the valued seemed to be constant. The secondary cracks achieved higher values of shear displacement due to its steeper inclination. The major cracks seem to be more perpendicular to the longitudinal direction, especially the ones that formed in the cross section near the application of the load.

The critical cracks were identified by analyzing the shear displacement results. These cracks presented an unstable behavior that triggered when the shear displacement reached a certain value, indicating the initiation of the opening of the critical inclined crack. The critical loads and critical shear displacements are given in Table 4. The values of critical shear displacements are similar for the beams that have the same cross-section (P804B1, P804A1, and P804A2). Beam P804A2 has a higher value because it was tested first in bending. The critical load could be used as a stop criterion since it is indicating the possible formation of irreversible damage and it represents a lower bound of the failure load, as shown in Table 4.

From Table 4, it can be observed that Lantsoght [13] found similar results by analyzing the deformation profiles determined with the values of the LVDTs measurements. The main addition is that DIC analysis allowed to determine the cracks kinematics during the failure process.

For most of the cracks, the crack width increased as the load level increased following an almost linear behavior until it reached a load where the value seemed to stay constant. The critical cracks presented a more unstable behavior.

To be able to apply a stop criterion, a measurable quantity should be chosen. Considering this, the most suitable response is the crack width at the reinforcement level, which can be measured during the test. The stop criterion based on shear displacement proposed by Yang [6] occurs after the formation of a crack. Therefore, it is convenient to choose a cross-section that is already cracked in bending. The bending crack develops more gradually and can be better monitored during a proof load test. The crack width of the first crack (Crack 1) that appeared, usually the one located near the point load, is chosen as possible stop criterion. The results are shown in Table 4.

# CONCLUSIONS AND RECOMMENDATIONS

This project deals with the assessment of the crack kinematics of four reinforced concrete beams without shear reinforcement to implement the critical shear displacement theory proposed by Yang [6]. This new model proposes that the opening of the critical crack can be considered as a lower bound for the shear capacity of a structural member. The unstable opening of the critical inclined crack is triggered when the shear displacement of an existing flexural crack reaches a critical value. Therefore, the critical shear displacement is used as a failure criterion. The shear displacements and crack openings were found using digital image correlation.

After assessing and analyzing the DIC results, the following conclusions and recommendations can be drawn:

- Out of the four beams considered, the beam P502A2 was the only one that showed good agreement between the results obtained from the DIC analysis and those obtained with the LVDTs in terms of horizontal displacements. The results of the other beams (P804B1, P804A1, and P804A2) presented a large scatter and it was not possible to make a comparison. This issue requires further investigation.
- The main issues for the correlation of images were that the painted pattern was not applied uniformly and that the position of the camera changed during the test.
   For further projects, it is recommended to avoid the latter and to ensure the application of a proper pattern to the surface of interest.
- Digital image correlation is an adequate technique to obtain refined measurements of the crack kinematics. In contrast to the traditional measurement methods, DIC allows to continuously track the evolution of each crack, even immediately before failure. Therefore it is possible to identify the moment of initiation of the opening of the critical inclined crack.
- For the beams with the same cross-section, the values for critical shear displacement were comparable. The value was around 0.4 mm.
- The critical load could be used as a stop criterion since it represents the initiation of irreversible damage and is a lower bound for the failure load, the range is between 84% and 92% of the failure load.
- To apply a stop criterion based on shear displacement, the crack width at the reinforcement level at the critical cross section was chosen as a measurable response to be applied in a proof load test. The values were comparable for the beams with the same cross-section, with a range between 0.20 to 0.31 mm.

With respect to a future research, a possibility could be to extend this analysis to beams with different dimensions and construct a database to improve the proposed expressions to obtain the critical shear displacements. The results of this project showed that the values are approximately 10 times bigger than the results calculated with the proposed expression (Eq. 13 or 14).

#### **REFERENCES**

- [1] Y. Yang, J. Walraven and J. Den Uijl, "Shear Behavior of Reinforced Concrete Beams without Transverse Reinforcement Based on Critical Shear Displacement," *Journal of Structural engineering*, vol. 04016146, pp. 1-13., 2016.
- [2] Y. Yang, C. van der Veen, D. Hordijk and A. de Boer, "The shear capacity of reinforced concrete members with plain bars," *Structural Faults and Repair 2016*, 2016.
- [3] ACI Committee 437, Code Requirenments for Load Testing of Existing Concrete Structures (ACI 437.2 M-13) and Commentary, Farmington Hills, MA, 2013, p. 24.
- [4] D. A. f. Stahlbeton, *DAfStb-Guideline:Load tests on concrete structures*, Deutscher Ausschuss für Stahlbeton, 2000, p. 7.
- [5] R. Koekkoek and Y. Yang, Measurement Report on the transition between flexural and shear failure of RC beams without shear reinforcement, Delft University of Technology, 2016.
- [6] Y. Yang, Shear Behaviour of Reinforced Concrete Members without Shear Reinforcement, A New Look to at an Old Problem, Delft: PhD Thesis, 2014.
- [7] Y. Yang, J. den Ujil and J. Walraven, "Critical shear displacement theory: on the way to extending the scope of shear design and assessment for members without shear reinforcement," 2016.
- [8] Y. Yang, J. A. den Ujil and J. Walraven, "Shear capacity of reinforced concrete beams under complex loading conditions," *Proc. 9th Fib Int. Ph.D. Symp. Karlsruhe Institute of Technology*, pp. 43-48, 2012.
- [9] J. C. Walraven, "Fundamental analysis of aggregate interlock," *J. Struct. Eng.*, no. 107(ST11), pp. 2245-2270, 1981.
- [10] E. Mörsch, "Der Eisenbetonbau [Concrete-steel construction]," *Engineering News Publishing*, 1909.
- [11] T. a. R. H. Bauman, "Versuche zum studien del verd"belungswirkung der biegezugbewehrung eines stahlbetonbalkens [Experimental study on dowel action in reinforced concrete beams]," *Deutscher Ausschuss für Stahlbeton (DAfStb)*, 1970.
- [12] E. Latsoght, *Development of a stop criterion for shear based on aggregate interlock*, 2017.
- [13] E. Lantsoght, Y. Yang, C. van der Veen and A. Bosman, "Analysis of beam experiments for stop criteria," Delft University of Technology, 2017.
- [14] E. Jones, *Documentation for Matlab-based DIC code*, Urbana-Champaign: University of Illinois, 2015.

А

# MATLAB-BASED DIC CODE

#### **MAIN GUIS**

To run these GUIs simply type the name of the GUI in the Matlab command window and press enter or select the GUI and press F9.

```
C:\Users\gzara\Desktop\CODES\Main.m
                                                                                    X
                                                                                         ⊙ 🛣
                                                           장등
                                                                                  a (?)
    EDITOR
                 PUBLISH
                                VIEW
                Tind Files
                             ♦ •
                                                                  Run Section
                Compare ▼
                             Go To ▼
     Open
                                                       Run
                                                           Run and
                                                                  Advance
           Save
                                            Breakpoints
                                                                               Run and
 New
                🚐 Print 🔻
                              Find 
            FILE
                              NAVIGATE
                                            BREAKPOINTS
 1
        %Main
        % Color photos
 2
 3 -
       reference_UC
 4 -
       UC Params
 5 -
       image_setup_GUI
 6
        % B&W photos
 7 -
       rotateIMG
 8 -
       correlate_images_GUI
       B_01_ResizeReduceGrid(20,2)
 9 -
10 -
       B 02 ResizeFullGrid(10)
11 -
       compute_data_GUI
12
13 -
       visualize_data_GUI
14 -
       UC_Params
15 -
       UC_Cracks
16 -
       clear all
17 -
       movie_GUI
18 -
       GZ Disp
19
20 -
       load('grid_data.mat')
21 -
       load('grid_reduced_data.mat')
22 -
       load('grid_setup.mat')
23 -
       load('grid_setup_reduced.mat')
24 -
       load('image setup.mat')
25 -
       load('disp raw data');
26 -
       load('corr_setup.mat')
27 -
       load('grid_setup.mat')
       load('grid_setup_reduced.mat')
28 -
29 -
       load('corr_setup_reduced.mat')
30 -
       load('DU data.mat')
       load('valid data')
31 -
32 -
        load('disp_reduced_data')
33 -
       load('FEM_setup.mat')
34
35 -
        save ('DATA9130')
36
37
                                             script
                                                                              Ln 15 Col 10
```

Figure A.1 Main GUIs

- 1. reference\_UC: Finds the angle and the scale of the photos
- 2. UC\_Params: Contains the parameters needed to run the GUIs rotateIMG, UC Cracks and UC LVDTs.
- 3. image\_setup\_GUI: Prepares the images changing them to black and white.
- 4. rotateIMG: Rotates images so the specimen is completely vertical.
- 5. correlate\_images\_GUI: Performs the image correlation and outputs displacements.
- 6. compute\_data\_GUI: Smooths and interpolates displacements, and calculates strains using finite element shape functions.
- 7. visualize\_data\_GUI: Displays displacements and strains
- 8. UC Cracks: Identifies the cracks, calculates strains, displacements and forces
- 9. GZ\_Displ: Calculates the displacements between a pair or more selected points.

#### STEPS FOR A TYPICAL CORRELATION

The steps for a typical correlation are explained below.

- 1. Prepare a folder that contains the selected images.
- 2. Open reference\_UC
  - a. Set the number of images to be evaluated
  - b. Write the name of the first photo
  - c. Change the range of RGB2 to match the set of photos
  - d. Change the distance between the red points (units in mm)

```
%% Part to find the angle and the scale of the photo
1
2
3 -
      global IMG X;
 4 -
      nFigure=0;
5
                       %number of images to evaluate
      form='jpg';
      sName1=sName;
10 -
      cali={};
11 -
      ini_refp=zeros(1,2);
12 -
      ini_refl={};
13 -
      ini theda=0;
14 -
      ini rl=zeros(1,2);
15 - For nPhoto=1:nPhotos
16
17 -
           sName1 (end-3:end) =num2str(str2num(sName(end-3:end))+nPhoto-1);
18 -
          IMG =imread( [sName1 '.' form]);
19
20 -
          if nPhoto==1
21 -
             RGB2 = [140 100 100]
22 -
               DISTORTION = [-2.769082e-013, 1.623054e-009, -2.990158e-006, 1.001618e+000, 1.339464e+000];
23 -
               nFigure=1+nFigure;
               figure (nFigure)
26 -
               title('Please mark the calibration area for the reference analyse.', 'Fontsize', 12);
27 -
28 -
               imshow(IMG)
29 -
               [bgc,ac,bc] = roipoly(IMG); %determine the reference area by the users
30 -
              hold off
31
32 -
33 -
              title('Please mark a vertical edge of the specimen.', 'Fontsize', 12);
34 -
              hold on
35 -
               imshow(IMG)
36 -
               [x,y] = ginput(2); %determine the reference area by the users
                   [\sim, \sim, nTheta]=evl([x, y], 2, 2);
37
38 -
               [nTheta, ~, ~] =aux 07 AngLCent([x(1) y(1)],[x(2) y(2)], 1);
39 -
               disp(['Theta:' num2str(nTheta) ' rad'])
40 -
              hold off
41
```

```
43
                nFigure=1+nFigure;
                figure (nFigure)
44
45
                imshow(gmultiply(uint8(bgc),IMG))
        ુ જ
                title(sName1)
46
47 -
            cali(nPhoto) = prep(bgc,ac,bc,RGB2,DISTORTION); %determine the coordinate of the markers in t
48
                clear IMG;
49 -
            disp([str2num(sName1(end-3:end)) nPhoto size(cali{nPhoto},1)])
50
51 -
            [ini_refp(nPhoto,:),ini_refl(nPhoto),ini_theda(nPhoto)] = evl(cali{nPhoto},3,3);
52 -
            length = [100 100];
ini_rl(nPhoto,:) = length./mean(ini_refl{nPhoto});
53 -
54 -
55
56 -
        nTheta=mean(ini theda);
57 -
        nScale=mean(ini_rl(:,2));
58
59 -
        nFigure=1+nFigure;
60 -
        figure(nFigure)
61 -
        subplot (1,2,1)
62 -
63 -
        semilogy(abs(ini_theda))
        grid on
64 -
        title('Angle Initial photos')
65 -
        subplot (1, 2, 2)
66 -
        semilogy(ini_rl(:,2))
67 -
        grid on
68 -
        title('Scale Initial photos')
69
70
71 -
        stop
72
73
```

Figure A.2 reference\_UC

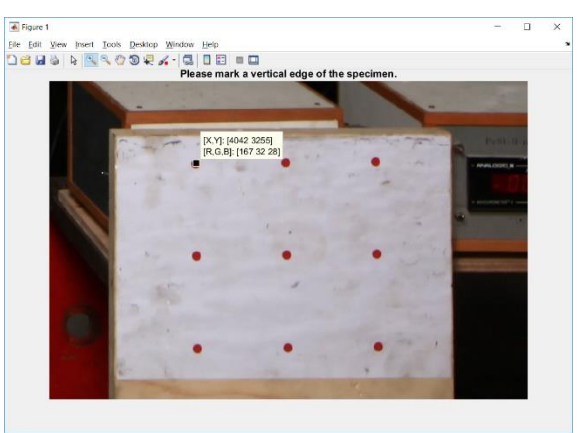


Figure A.3 Example of RGB values

3. Run *reference\_UC* to find the angle and the scale a. Select the area that contains the red points

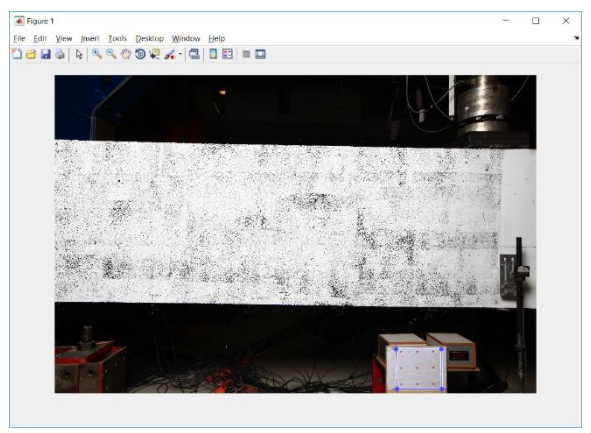


Figure A.4 Area containing the red points

b. Mark a vertical or horizontal edge of the specimen



Figure A.5 Marking of the horizontal edge of the specimen

c. The angle and the scale of the photos will be shown in a plot

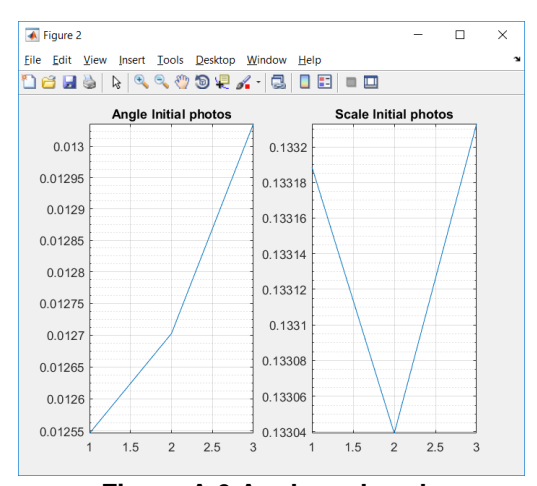


Figure A.6 Angle and scale

- 4. Run image\_setup\_GUI to prepare the images
- 5. Open UC\_Params
  - a. Change the values of *Param.nScale* and *Param.n.Theta* to the corresponding values to the group of photos and evaluate them.



Figure A.7 UC\_Params photo parameters

- 6. Run *rotateIMG to rotate the photos* **Note:** If the angle between the pictures differs a lot, problems in the correlation of the picture might appear.
- 7. Run correlate\_images\_GUI
  - a. Type of loop → Parallel

b. Reduced images → Correlate reduced images? → YES
 Note: Choose a large subset size and a sparse grid to start the iterations.

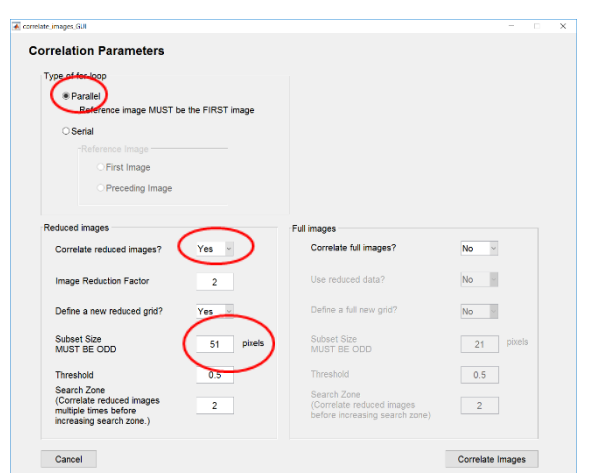


Figure A.8 Correlation Parameters for reduced images

- 8. Run visualize\_data\_GUI
  - a. Image skip → 1
  - b. Choose Reduced data
  - c. Displacement →Smoothed/interpolated
  - d. Click on Filled Contour Plot

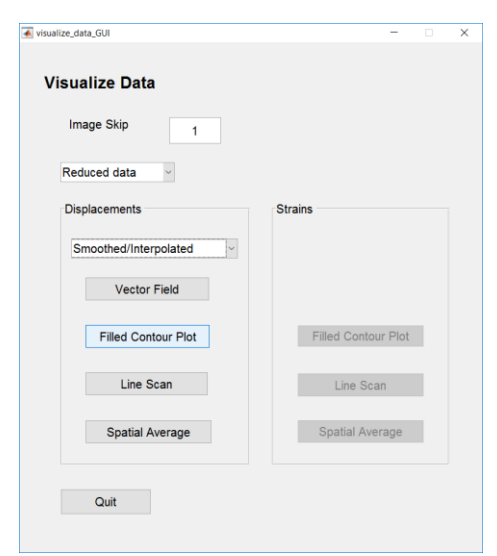


Figure A.9 Options for visualizing the reduced data

- e. Which data do you want to plot? →Magnitude of Displacements
- f. Scale of the plot→ Automatic scale
- g. Click on View Contour Plot

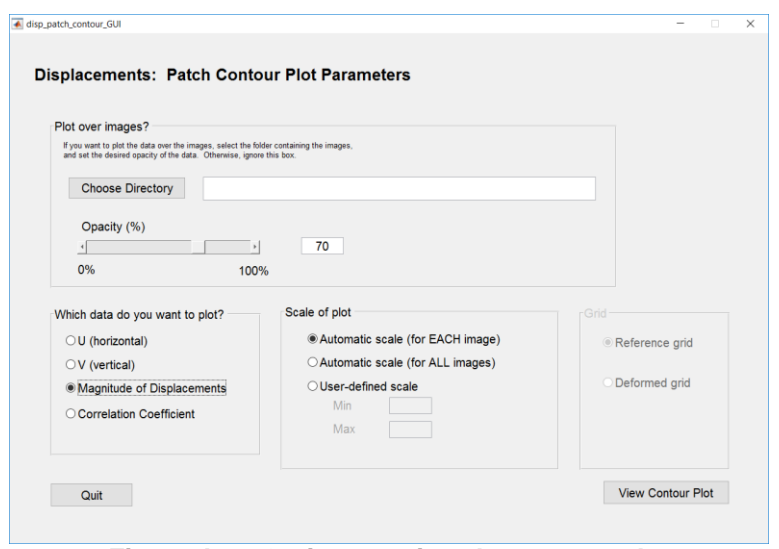


Figure A.10 Options to view the contour plot

- 9. Run correlate\_images\_GUI
  - a. Type of loop  $\rightarrow$  Parallel
  - b. Full images→ Correlate full images? →Yes
     Note: Choose a smaller subset size and denser grid

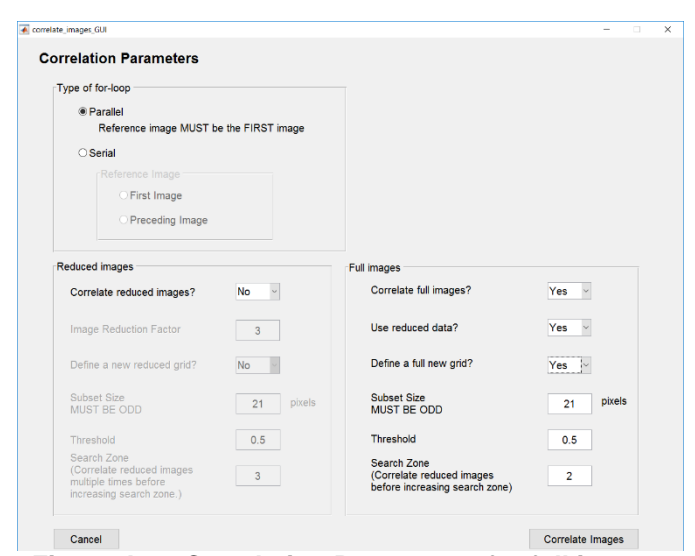


Figure A.11 Correlation Parameters for full images

- 10. Run visualize data GUI
  - a. Image skip →1
  - b. Choose Full data
  - c. Displacements  $\rightarrow$  Smoothed/interpolated
  - d. Click on Filled Contour Plot



Figure A.12 Options for visualizing full data

- e. Which data do you want to plot? → Magnitude of Displacements
- f. Scale of the plot→ Automatic scale
- g. Click on View Contour Plo

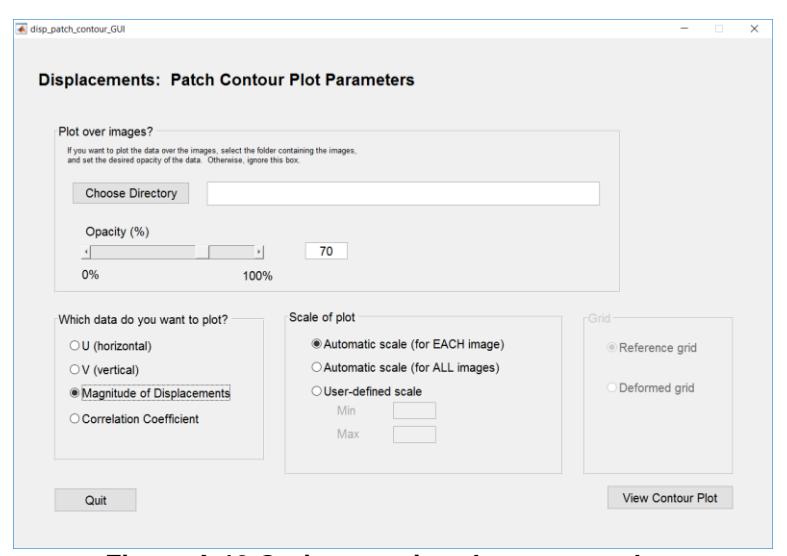


Figure A.13 Options to view the contour plots

**Note:** Check that the chosen subset size and grid display the full image, if not change the values and repeat the steps.

- 11. Run compute\_data\_GUI
  - a. Type of loop→paralllel
  - b. Strains algorithm  $\rightarrow$  Linear (4-node)



Figure A.14 Compute data parameters

- 12. Run visualize\_data\_GUI
  - a. Image skip →1
  - b. Choose Full data
  - c. Strains → Filled Contour Plot

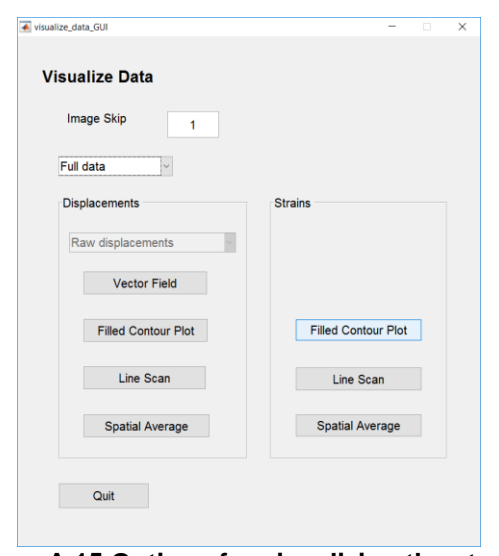


Figure A.15 Options for visualizing the strains

- d. Choose directory → Choose the folder where the photos are saved
- e. Which data do you want to plot?  $\rightarrow$ Infinitesimal strain  $\rightarrow$  e\_eqv
- f. Click on View Contour Plot

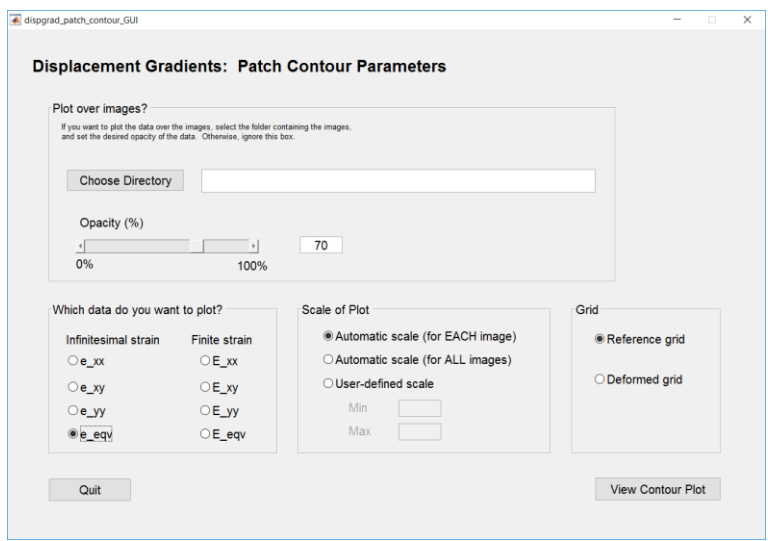


Figure A.16 Options to view the strains contour plot

- 13. To filter the images and identify the cracks, the following parameters must be changed until the cracks are fully grouped and filter.
  - a. Open UC\_Params and change the values

```
%Parameters for the filtering of the images
13 - Param.nThreshold=.05; %mean (less->more pixels)
14 - Param.nDisp=1.8; %Dispersion of the pixels (more->more pixels)
15 - Param.nFactorStd=.7; %Std (less->more pixels)
16 - Param.nVprt=22; %Std
17 - Param.nHprt=50; %Std
```

Figure A.17 Parameters for the filtering of images

Note: These values must be changed/checked for each of the pictures

**Table A 1 Function of parameters** 

Parameter	Function	
Param.nThreshold	Uses mean values, lower value = more pixels	
Param.nDisp	Uses the dispersion, lower value = more pixels	
Param.nFactorStd	Uses the standard deviation, lower value= more pixels	
Param.nVprt	Number of divisions in the vertical direction	
Param.nHprt	Number of divisions in the horizontal direction	

- 14. Run *UC\_Cracks* to obtain the forces and displacements on the cracks
  - a. Change number of the photo to the desired

```
X
C:\Users\gzara\Desktop\CODES\UC_Cracks.m
                                                                                   П
                                                                                  ?
                PUBLISH
                               VIEW
                                                           <u>과</u> 등
                                                                                        ⊙ ⊼
   EDITOR
                👼 Find Files
                                                                 Run Section
                Compare 🔻
                             🖒 Go To 🔻
                                                                 Advance
                                                          Run and
                                                                             Run and
 1
 2
        %% Identifying cracks
 3
 4
        %pass DATA from vector to matrix
 5
 6
        % aux_V2M(Vect,r,c)
 7 -
        nR=length(unique(gridy_DU));
 8 -
        nC=length(unique(gridx_DU));
 9 -
        vVect=small_strain.eeqv(:,48);
        mData=aux_V2M(vVect,nR,nC);
10 -
11
12
        % mData(370:end,920:end)=0;
        % mData(250:end, 330:end)=0;
13
14 -
        mData(isnan(mData))=mean UC(mData(:))*3;
15
        % % mData(isnan(mData))=max(mData(:));
16
17
        %Plot
18
19 -
        figure(1)
20 -
        clf
21
        % % [vH1,vV1,mData aux]=E 08 PrepSurf(unique(gridx DU)'-gridx DU,...
22
                unique(gridy_DU)'-gridy_DU, mData);
23
        % % vH1=vH1/vH1(end)*size(mData,2);
24
        % % vV1=vV1/vV1(end)*size(mData,1);
25
26
27
        % % surf(vH1, vV1, mData_aux)
28
        % % shading flat
        % % colormap jet
29
        % % axis([vH1(1) vH1(end) vV1(1) vV1(end)])
30
        % % view([0 0 -1])
31
32
                                                                              Ln 1
                                                                                     Col 1
```

Figure A. 18 UC\_Cracks

UC Cracks contains several functions and test, some of them will be explained:

## A 00 Crack

Function to clear and group the cracks

#### A 01 CrackLine

Function to find in each row the position of the crack

## A 02 Contour

Function to obtain the coordinates of the displacements in pixels near the crack.

 $R \rightarrow$  Parameter that refers to the distance from the crack to the point of recollection of data. Units in pixels

 $extit{MData} 
ightarrow ext{Matrix}$  that contains the information of displacements. Units in pixels

## A\_03\_DispContour

Function to find the coordinates of the contour of the crack and the displacements in pixels and outputs the displacements in mm

 $mW \rightarrow 2x2$  matrix that contains the weights to interpolate the displacements  $nScale \rightarrow Scale$  to convert from pixels to mm  $uData.Dispx.data \rightarrow Information on displacements. Units in mm$ 

## A 04 LocalDeltaTau

A function that adopts the contour of the crack and outputs the displacements to the right and left side of the crack.

 $nAng \rightarrow \text{Refers}$  to the angle of the cracks profile, changes at every position along the crack. Units in radians.

Delta→Displacement perpendicular to the crack profile

Delta= (Left-Right) \*-1

Tau→Displacement parallel to the crack profile

Tau= (Left-Right) \*-1

## A\_05\_LocalSigmaTau

A function that inputs the calculated displacements and outputs the stresses in the crack. Analytical shear stress from Walraven

```
da \rightarrowsize of the aggregates. Units in mm wo \rightarrowDelta do \rightarrowTau
```

## A\_07\_FxFy

A function that takes the stresses along the crack and outputs the forces in the vertical and horizontal direction. Aggregate interlock

## A 07 DwAction

Function to get the dowel action force

## Test 01

Plot cracks early stage

#### Test 04

Plot the distance of the cracks (Crack Spacing)

## Test 06

Plot the values of strains in the cracks

#### Test 07

Plot of the displacements along the crack profile and the projection of the difference between the left and right side of the crack

*Delta* → shear displacement W→ crack width

## Test 08

Plot of the stresses along the crack profile

#### Test 09

Plot of the cracks and the forces (Aggregate interlock)

## Test 14

Plot of the cracks and the forces adding the value of dowel action force contribution

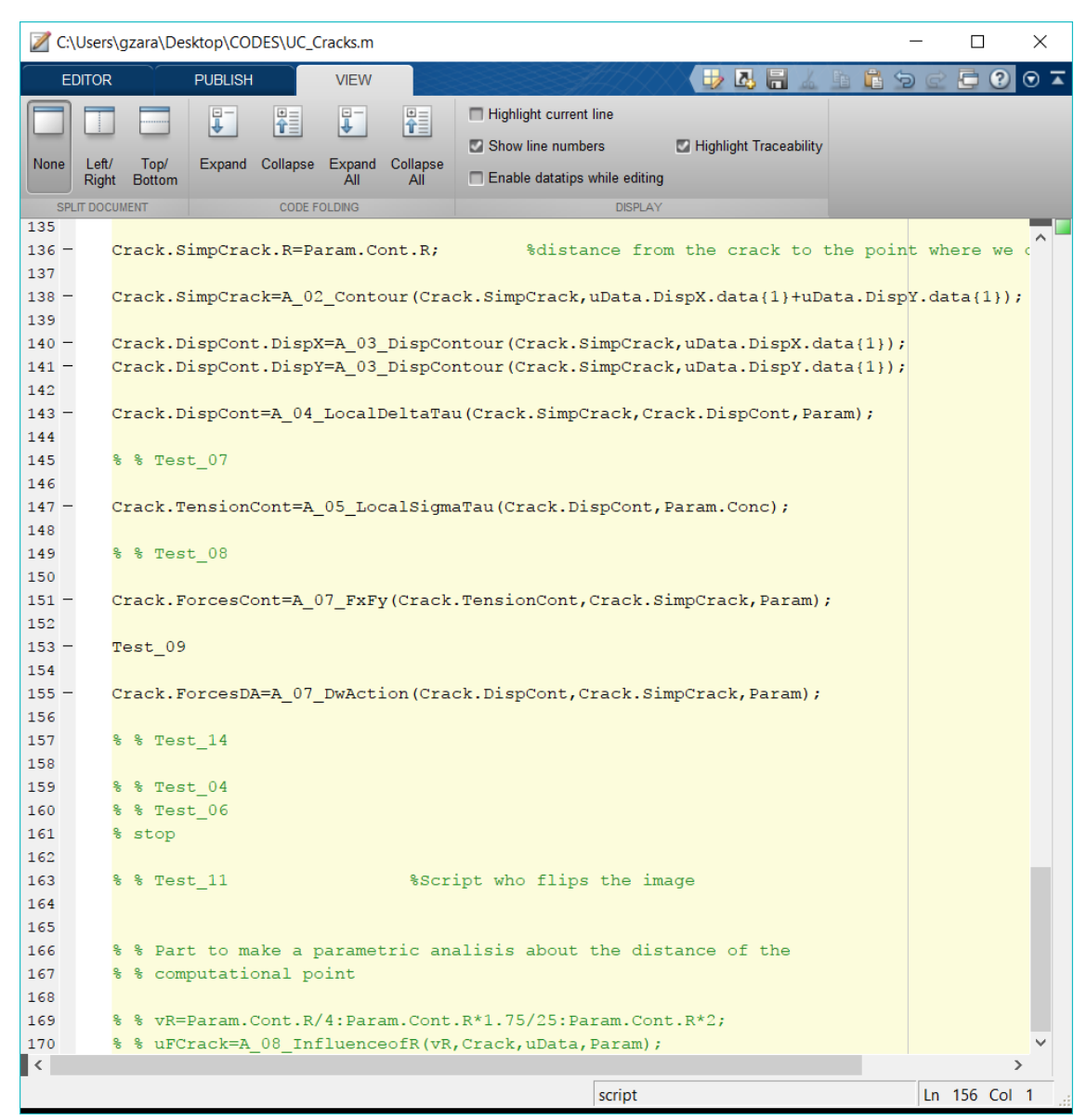


Figure A.19 UC\_Cracks functions and tests

In the following table, a summary of some useful variables and its place in the workspace is given.

**Table A.2 Variables located in Crack structure** 

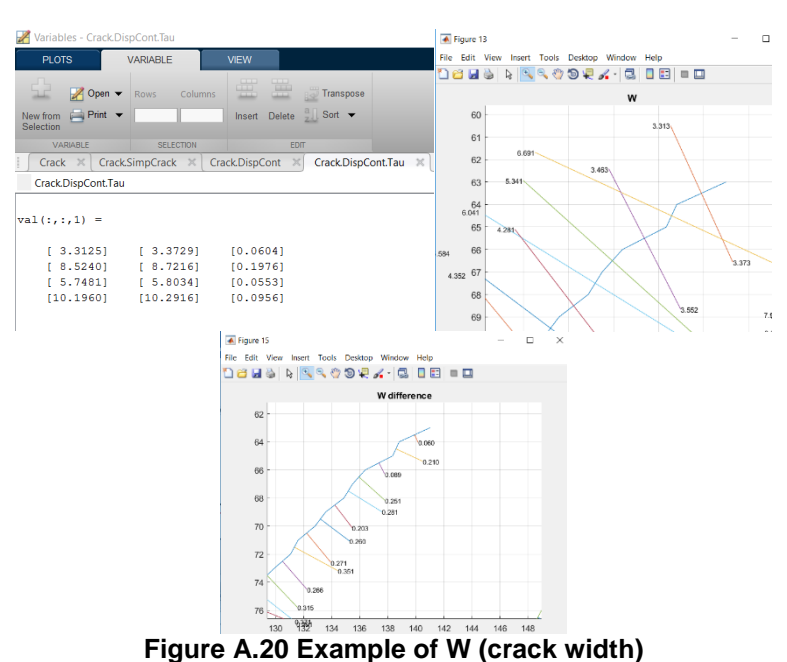
Crack	nFis	
	nPix	
	mFis	
	mlmg	
	Ang	
	mLog	
	mLogCntr	
	nAnglMed	
	Sep	
	uContour	
	mDistance	
	SimpCrack	mFis, mFisT, mFisCent, vAng, vL, vCent, R, mFisCont
	DispCont	DispX, DispY, Delta, Tau
	TensionCont	Sigma, Tau, Model
	ForcesCont	FCrack, X, Y
_	ForcesDA	DispY, fy, Cent

 $Crack \rightarrow SimpCrack \rightarrow mFis \rightarrow coordinates of the crack$ 

 $Crack {\longrightarrow} \ SimpCrack {\longrightarrow} \ mFisCent {\longrightarrow} \ center \ of \ the \ crack$ 

Crack→SimpCrack→vAng→ coordinates of the angle

 $\mathsf{Crack} {\to} \, \mathsf{DispCont} {\to} \, \mathsf{Tau} \, {\to} \mathsf{W} \, \, (\mathsf{crack} \, \, \mathsf{width})$ 



#### Crack→DispCont→ Sigma → Delta

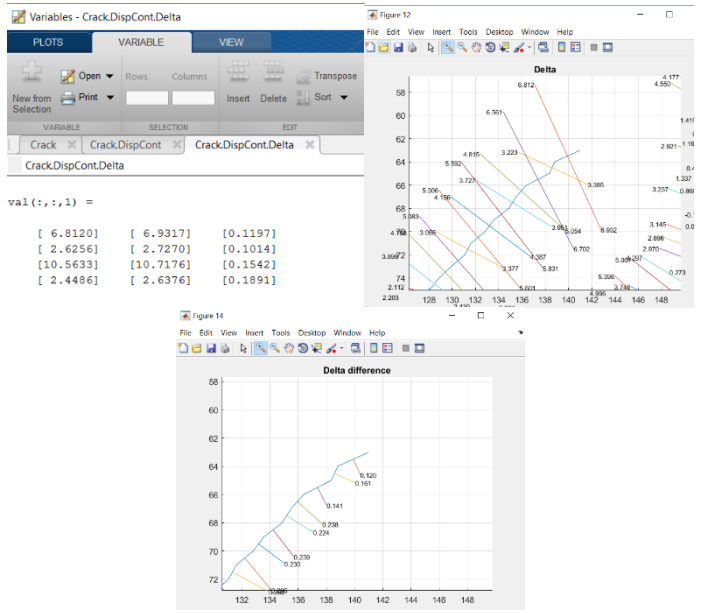


Figure A.21 Example of Delta

#### Crack→ ForcesDA→ fY → Dowel Action

- 15. Open GZ\_Displ
  - a. Load the desired correlated data
  - b. Choose the number of pair of points
  - c. Write the name of the picture chosen as background to pick the right points

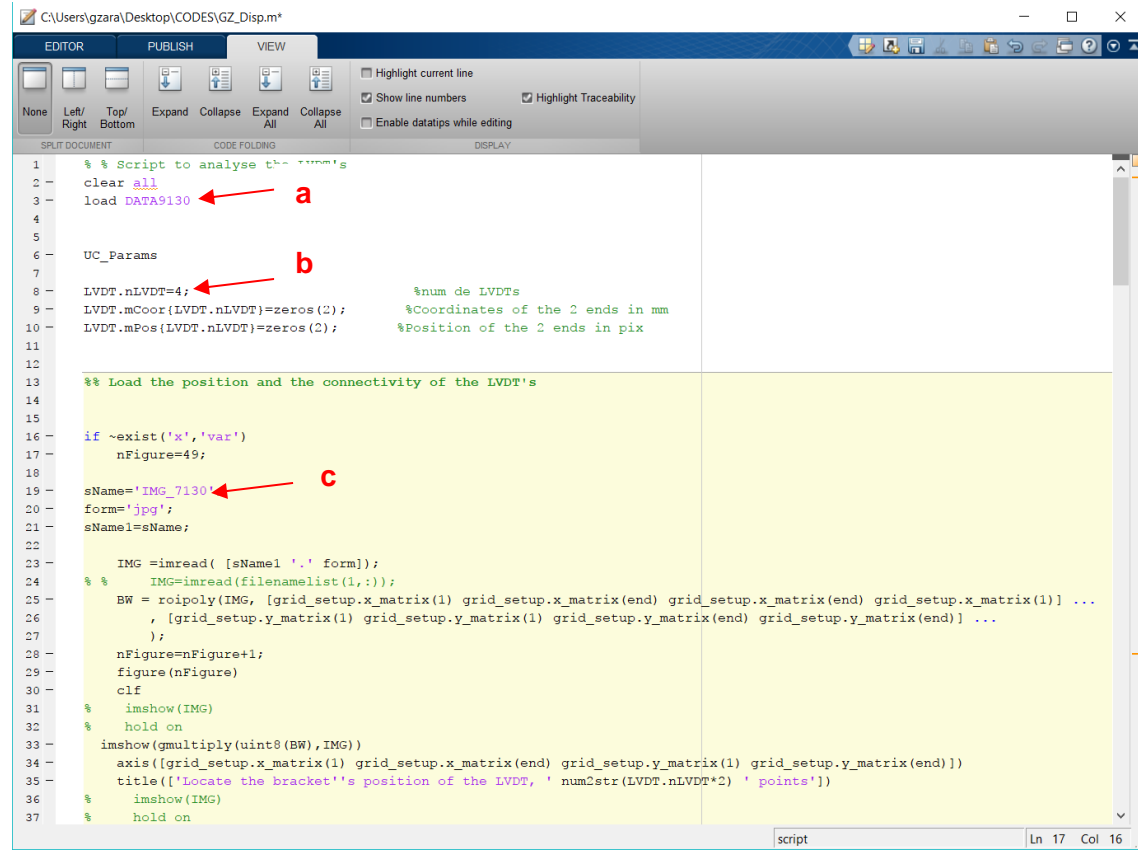


Figure A.22 GZ\_Displ

The information of the magnitude of the displacements for the picked points is given in:

Table A.3 Variables located in LVDT structure

LVDT	nLVDT	
	mCoor	
	mPos	
	mXY	
	mW	
	Displ	
	NaNs	
	Def	Ref, X, Y, XY, LineX & LineY

 $LVDT \rightarrow Def \rightarrow X \text{ or } Y$ 

## **B.1 RESULTS P502A2**

In total 34 pictures were correlated to obtain the results for the digital image correlation analysis. The reference image was taken before the test started, then 3 pictures were taken at every load step. The three pictures were taken with a difference of 2 seconds between each one and the last picture was taken 2 seconds before the failure.

The test of beam P502A2 resulted in a flexural failure at 148 kN.

## **B.1.1 LOADING SCHEME P502A2**

The total number of steps used for this test was of 10, including the unloading procedure done 3 times. The loading scheme measured during the experiment and the one obtained from the pictures used for the digital image correlation is given in Figure B.1.

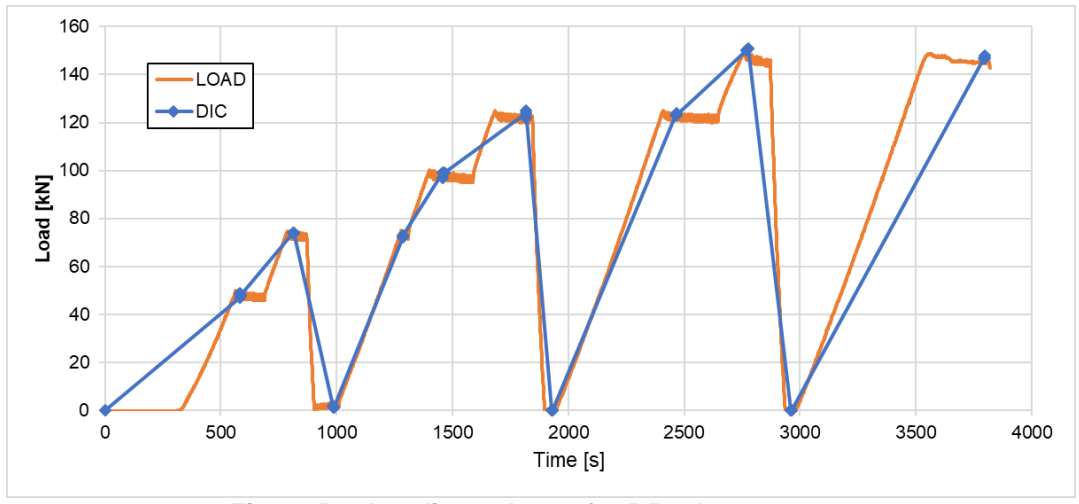
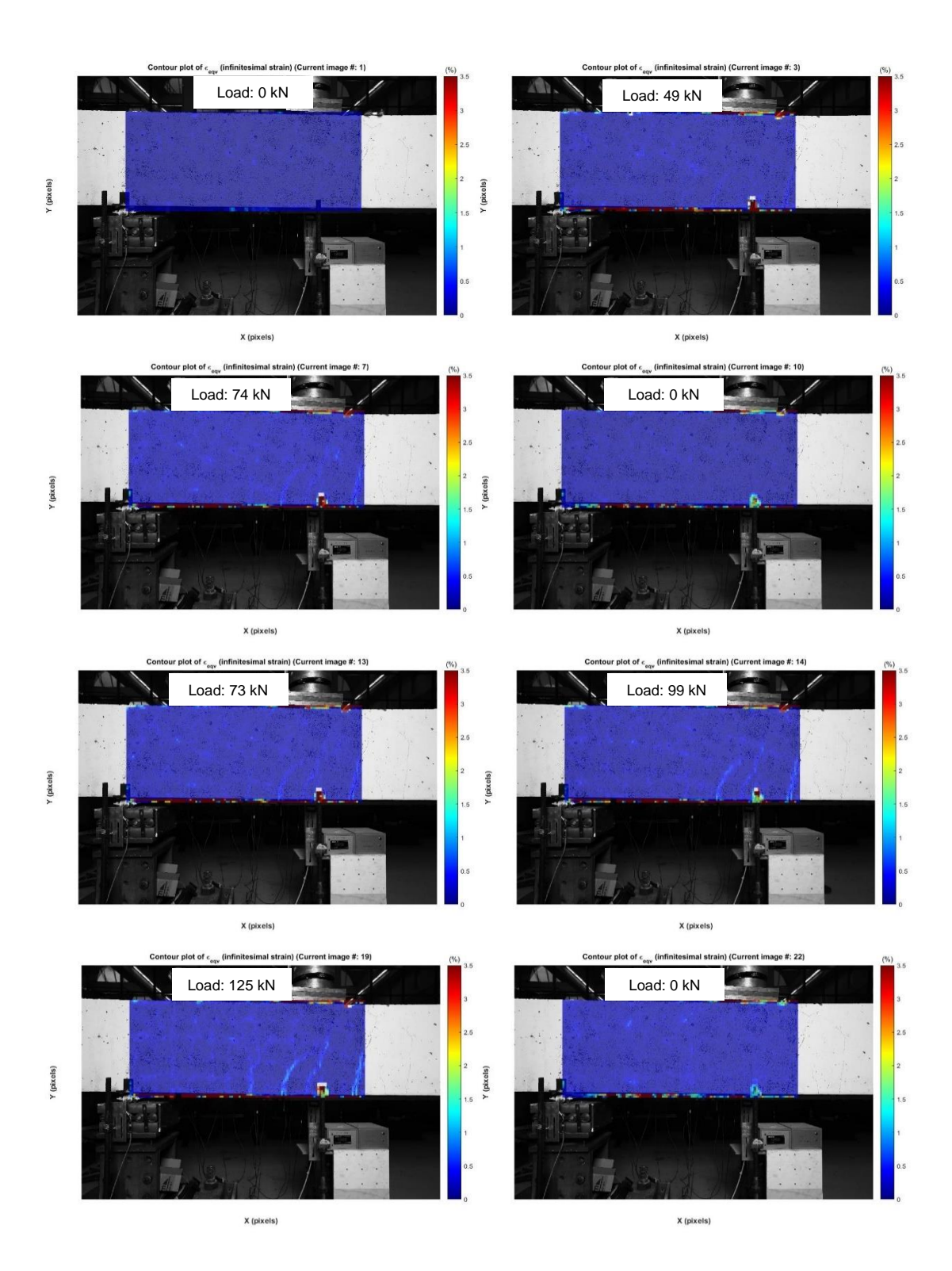


Figure B.1 Loading scheme for P502A2

## B.1.2 DIC RESULTS P502A2

For the DIC analysis, the final subset size used for this group of pictures was of 71 pixels with a grid equal to 30. In Figure B.2, the results for the representative load steps are shown. The pictures clearly show the evolution of the profile of the cracks. It can be observed that the first crack is visible at the first load step of 74 kN and that the failure occurs at a load level of 148 kN.



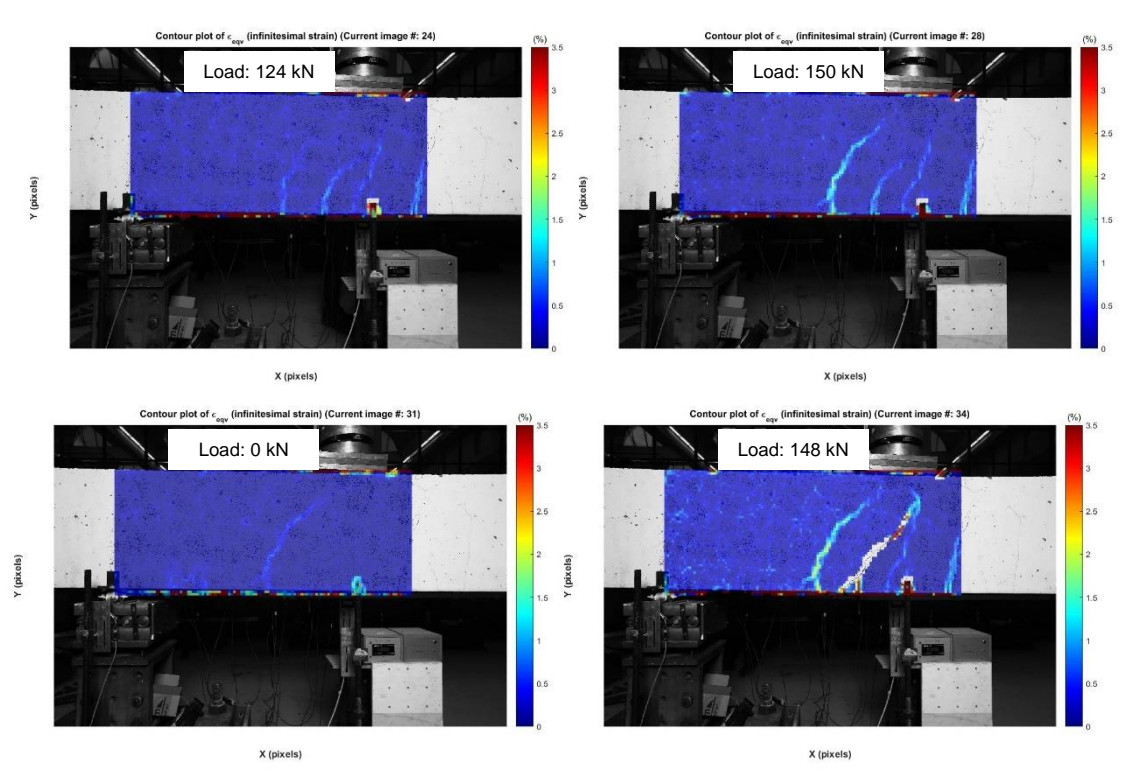


Figure B.2 DIC results for P502A2

## **B.1.3 MEASURED HORIZONTAL DEFORMATIONS P502A2**

The scale for this test was of 0.3473 mm/pix. In Figure B.3, the LVDTs location is shown, as well as the drawn array used for the comparison.

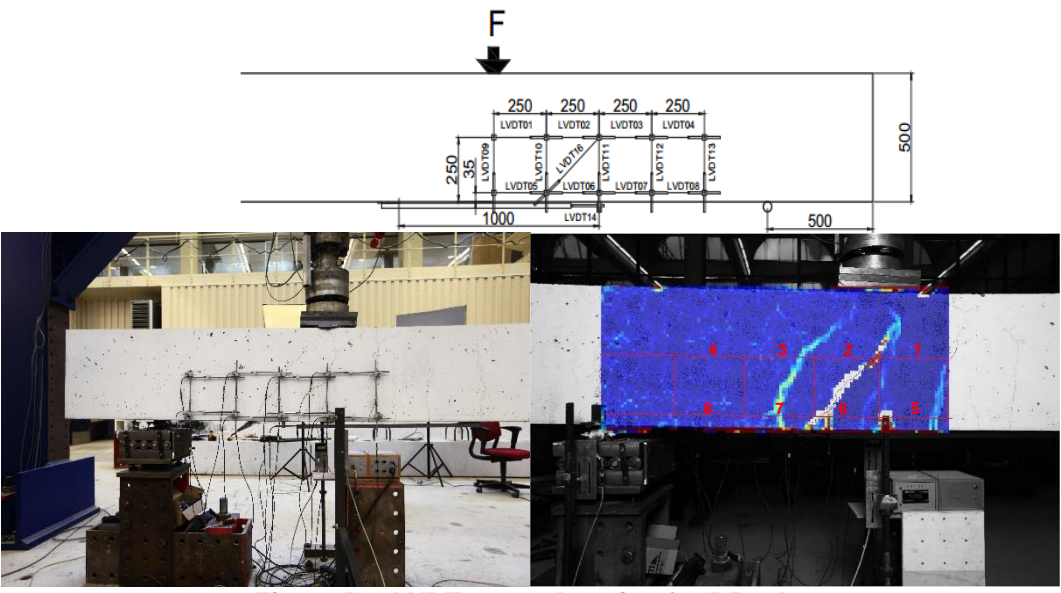


Figure B.3 LVDTs array location for P502A2

Figure B.4 shows the comparison of the results obtained for the horizontal deformation at the tensile reinforcement level.

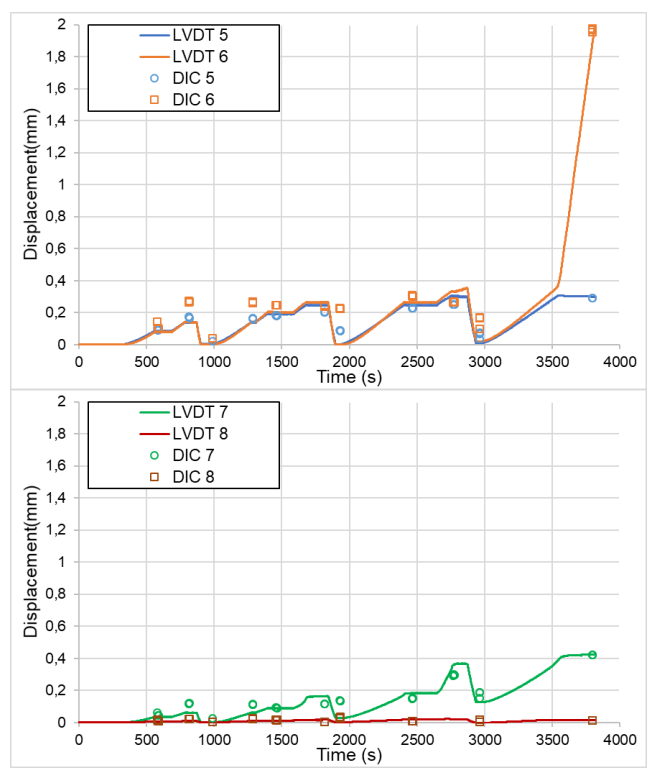


Figure B.4 Comparative of the horizontal deformation development of LVDT's 5-8 & DIC (bottom row) for P502A2

The results of horizontal displacements from DIC analysis agree well with those obtained with the LVDTs. For instance, the value obtained from the DIC measurements at a time of 3796s is equal to 1.95 mm against the LVDT value of 1.87 mm for LVDT 6.

# B.1.4 CRACK WIDTH ( $\Delta_X$ ) AND SHEAR DISPLACEMENT ( $\Delta_Y$ ) P502A2

The DIC results for picture 34 were used as background and the reinforcement level was drawn to help with the selection of points at the left and right side of the cracks, as it can be observed in Figure B.5.

Four major cracks were identified (Figure B.5).

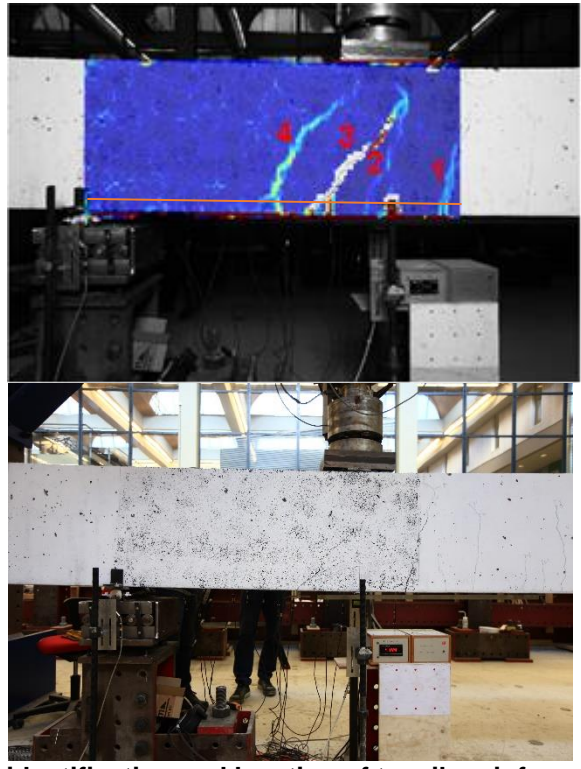


Figure B.5 Crack identification and location of tensile reinforcement for P502A2

Figure B.6 shows the plot constructed with the values of shear displacement against the measured load. It can be observed, as expected, that the shear displacement increases as the load level increases and that the behavior at the load step of 124 kN and onwards is slightly different from the previous load steps.

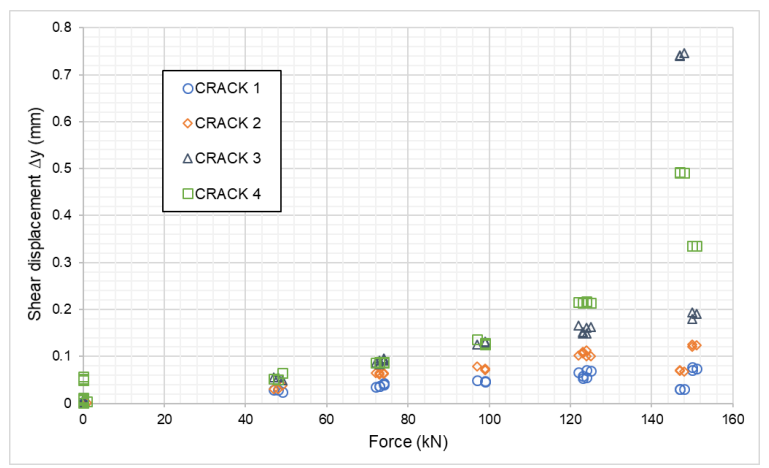


Figure B.6 Shear displacement for major cracks for P502A2

After analyzing these results, it was concluded that cracks 3 and 4 are the critical cracks. In Figure B.7, the red continuous line represents the load level from which the observed general behavior of the shear displacements triggers. The value is equal to 124 kN, that represents the 85% of the failure load. At this load level, the shear displacement could be identified as the critical shear displacement. The value is equal to 0.21 mm.

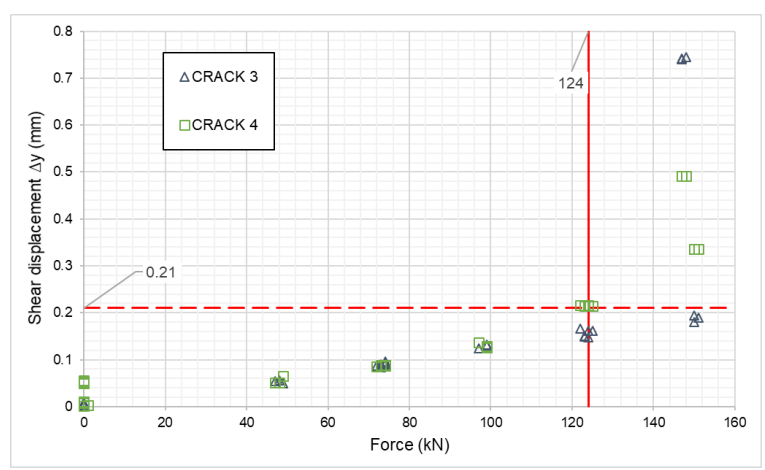


Figure B.7 Critical inclined cracks and critical shear displacement for P502A2

Figure B.8 shows the plot constructed with the values of crack width against the measured load. As expected, the crack width increases as the load level increases. The same behavior of the shear displacement can be identified.

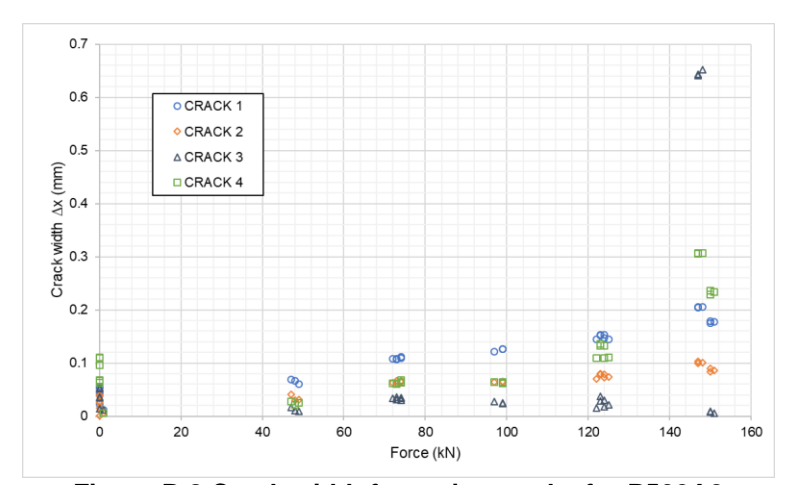


Figure B.8 Crack width for major cracks for P502A2

The results of crack width for Crack 1 were analyzed and the crack width identified for the load step of 180 kN was of 0.15 mm.

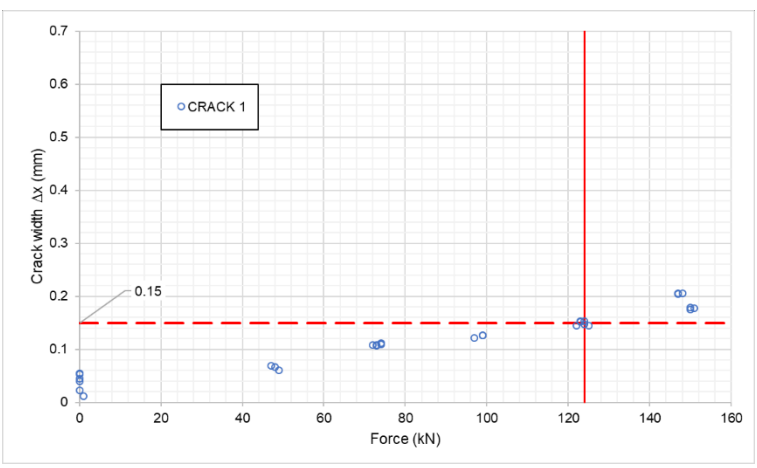


Figure B.9 Crack width for Crack 1 P502A2

## **B.2 RESULTS P804A1**

In total 68 pictures were correlated to obtain the results for the digital image correlation analysis. The analysis was divided into two parts since the position of the camera changed during the test. For the first part, 30 images were correlated and for the second 38.

The reference image was taken before the test started, then approximately 2 pictures were chosen at every representative load step. Since the scale of the pictures changed, a continuous DIC analysis was not possible. To solve this problem, the last DIC results for the first part of the analysis was added to the second part.

The test of beam P804A1 resulted in a flexural failure at 207 kN.

## **B.2.1 LOADING SCHEME P804A1**

The loading scheme for this test consisted of a total number of 42 cycles, where 8 load levels were studied. Figure B.10 shows the results obtained during the test and the DIC analysis.

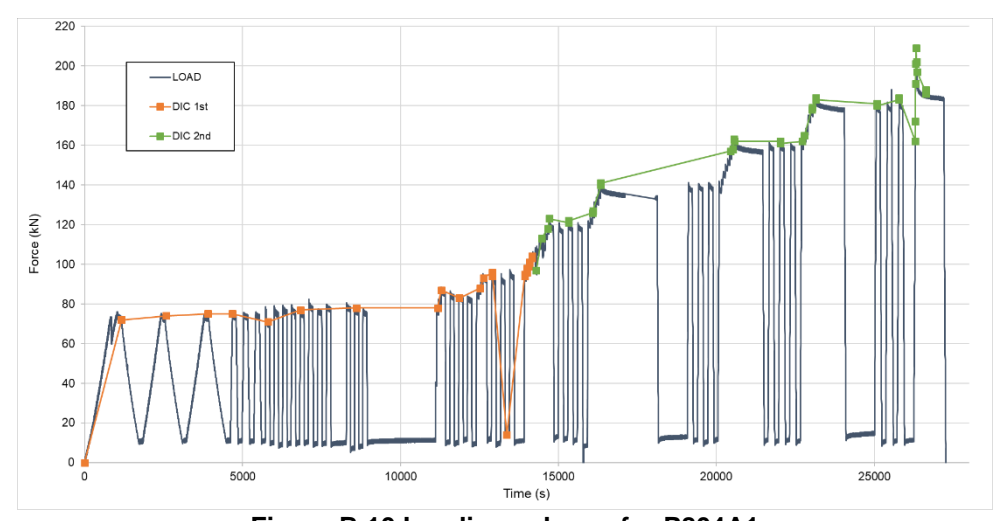


Figure B.10 Loading scheme for P804A1

## B.2.2 DIC RESULTS P804A1

For the first part of the DIC analysis, the subset used was of 121 pixels with a grid equal to 30. In Figure B.11, the results for the representative load levels are shown. It can be observed that a crack starts to be visible at the load step of 78 kN. However, it is important to note that the crack is not well defined.

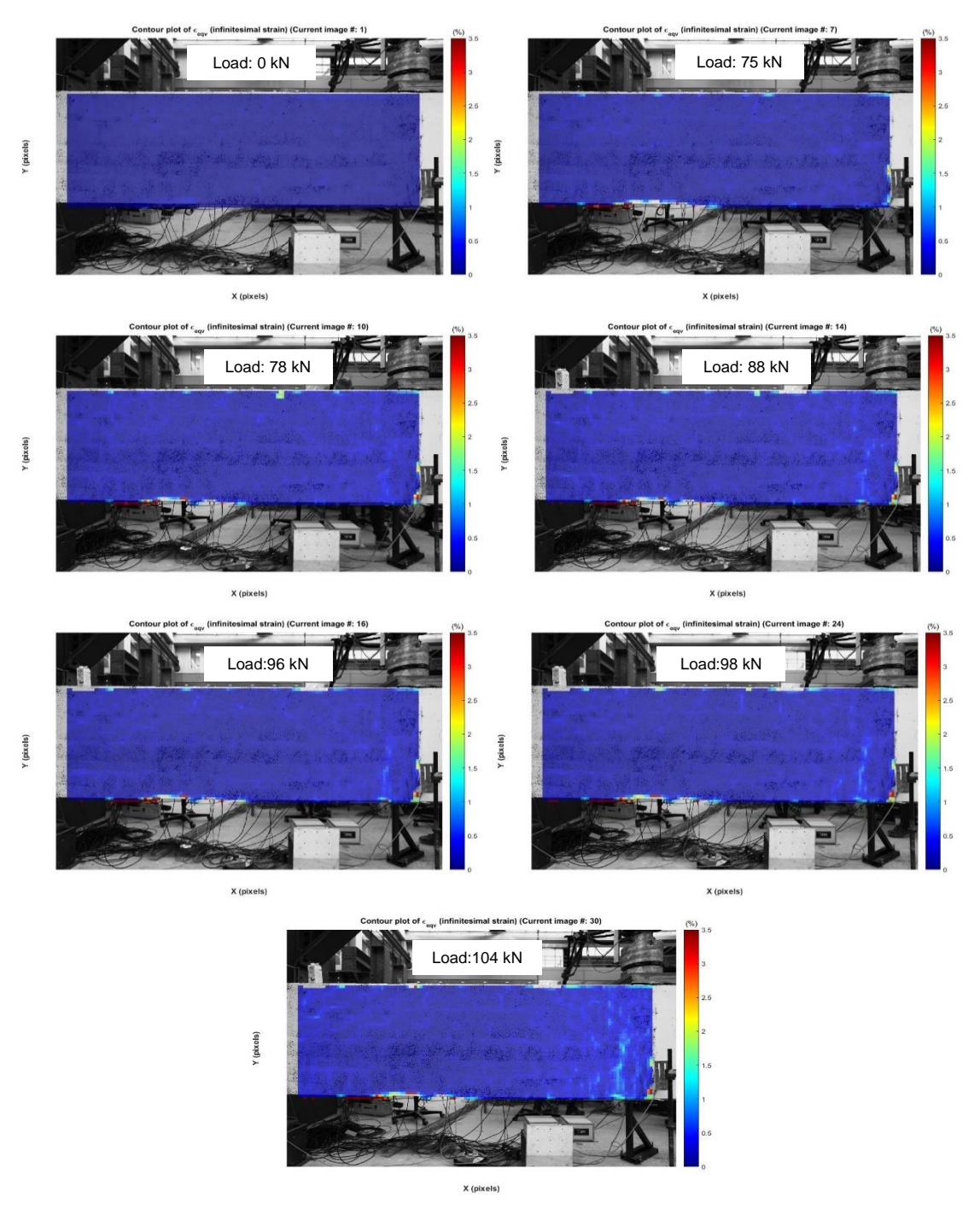
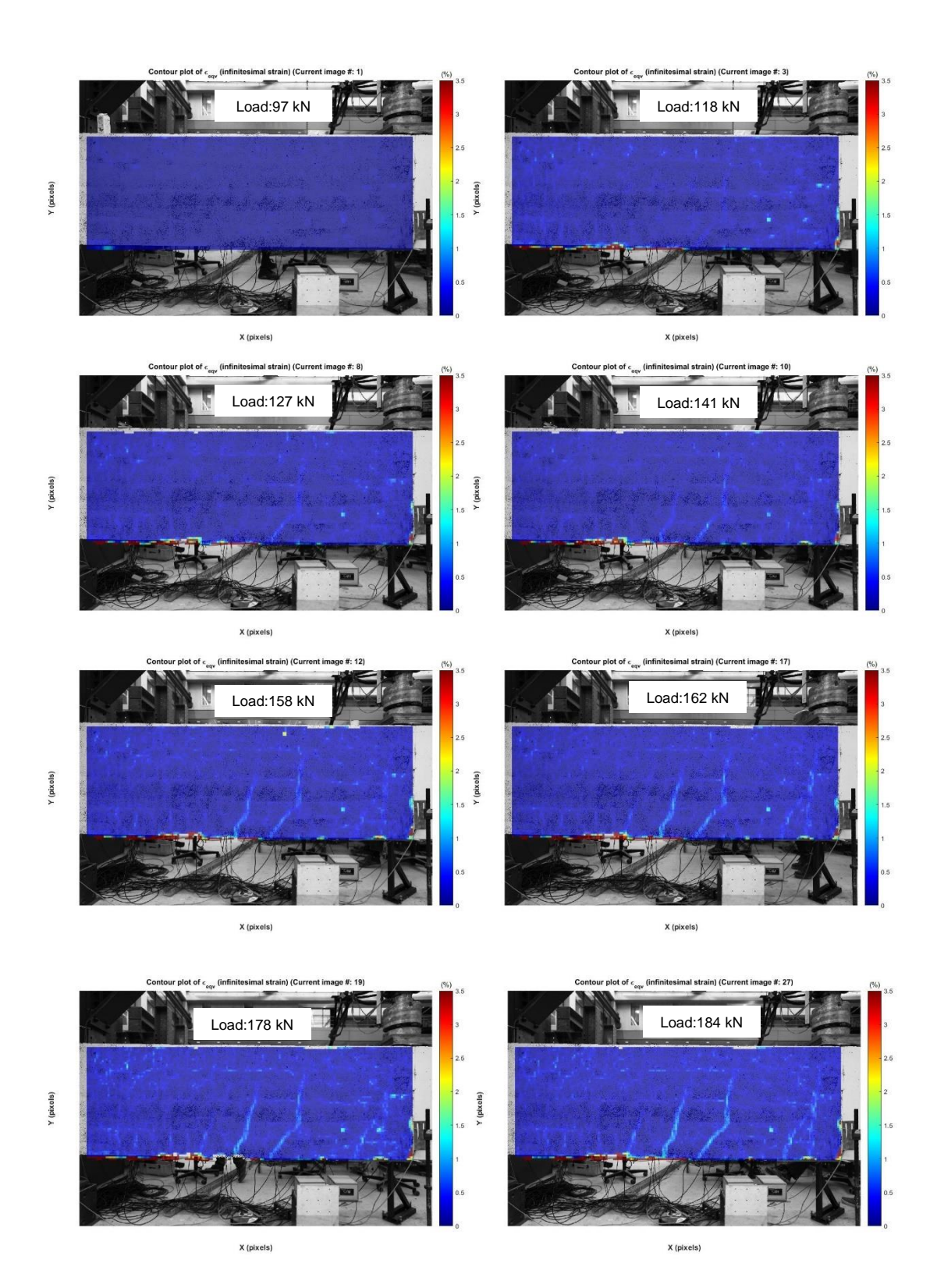


Figure B.11 DIC results for representative load levels for P804A1-1 (First part)

The results for the second part of the DIC analysis are shown in Figure B.12. The subset size used was of 91 pixels with a grid of 30. The reference image was the picture taken at the load step of 97 kN. Four more flexural cracks developed for this second part of the test.



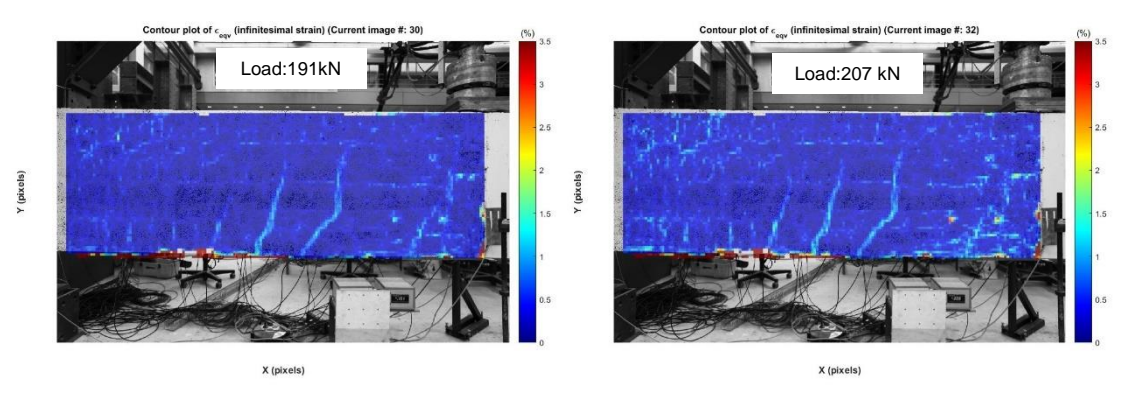


Figure B.12 DIC results for representative load levels P804A1-2 (Second part)

The DIC results of this test did not correlate well.

## **B.2.3 MEASURED HORIZONTAL DEFORMATIONS P804A1**

The scale used for the first part of the DIC analysis was of 0.4570 mm/pix and for the second part 0.4541 mm/pix. In Figure B.13, the LVDts location is shown, as well as the drawn arrays used for both parts of the DIC analysis.

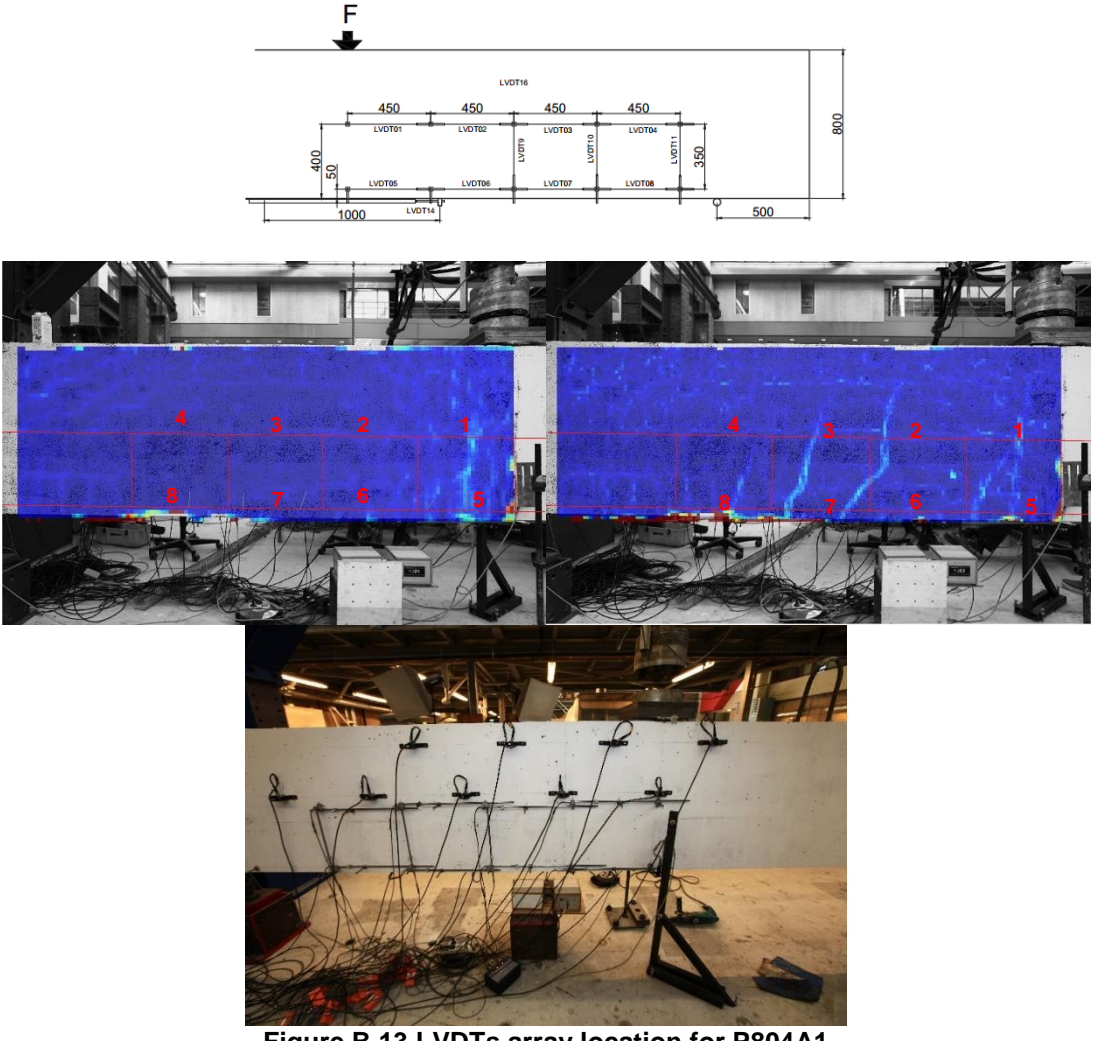


Figure B.13 LVDTs array location for P804A1

Figure B.14 shows the comparison of the results obtained for the horizontal deformation at the tensile reinforcement level. The DIC results were obtained by adding

the values from the last correlated picture of the first part of the analysis to the results of the second part.

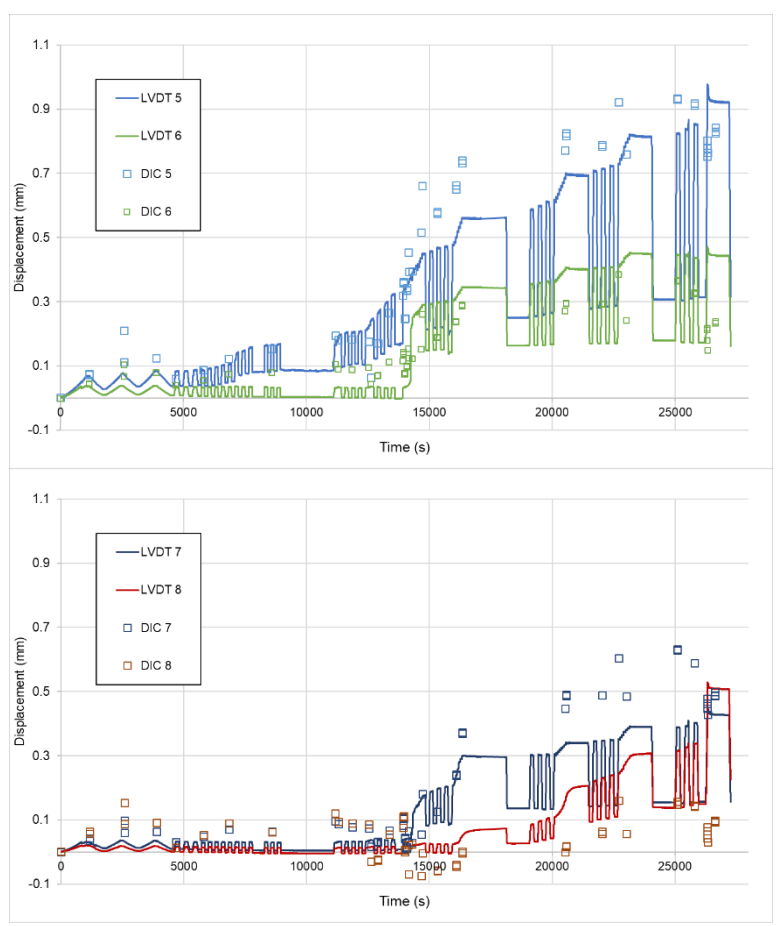


Figure B.14 Comparative of the horizontal deformation developments of LVDT's 5-8 & DIC (bottom row) for P804A1

The results from the DIC analysis differ from the LVDTs measurements, especially for the second part of the analysis, from the time equal to 14299s and onwards. However, the same behavior can be observed for both measurements with the difference that the values found with the DIC are higher for LVDTs 5 and 7 and lower for the LVDTs 6 and 8.

As mention in the previous section, the position of the camera was changed during the experiment, which hindered the process of correlation and this is reflected in the results for the second part.

# B.2.4 CRACK WIDTH ( $\Delta_X$ ) AND SHEAR DISPLACEMENT ( $\Delta_Y$ ) P804A1

Figure B.15 shows the pictures used as background for the selection of points at the left and right side of the cracks. To get the displacements of the cracks at the first part of the analysis, the location of the cracks was identified and localized in the picture.

Three major cracks (1,3 & 4) and two secondary cracks (2 & 5) were identified.

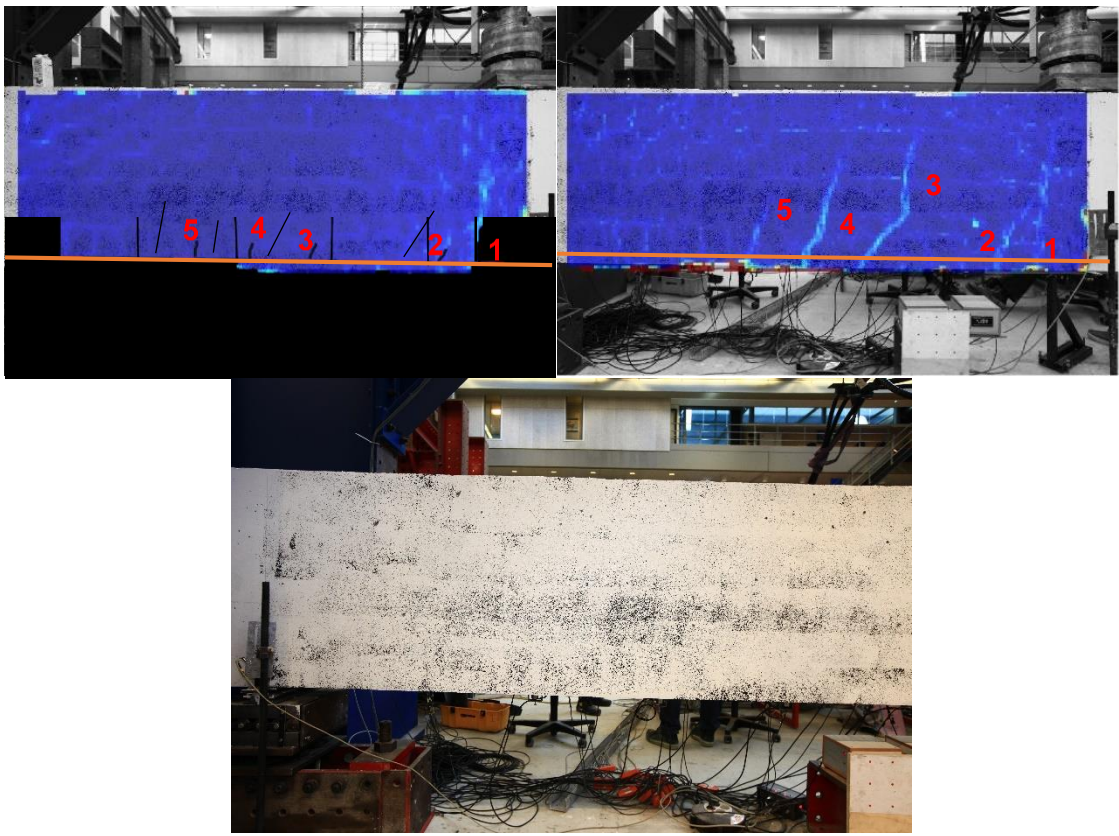


Figure B.15 Crack identification and location of the tensile reinforcement for P804A1

The following pictures present the plots of shear displacement vs load. Figure B.16 and Figure B.17 show the results of the major cracks and secondary cracks respectively.

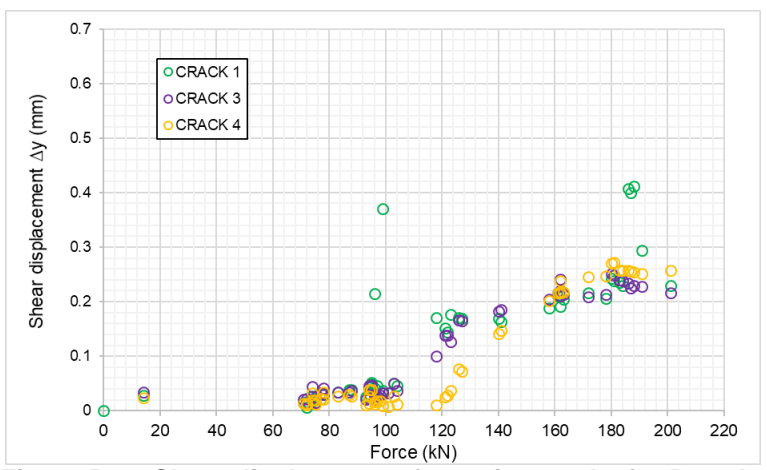


Figure B.16 Shear displacement for major cracks for P804A1

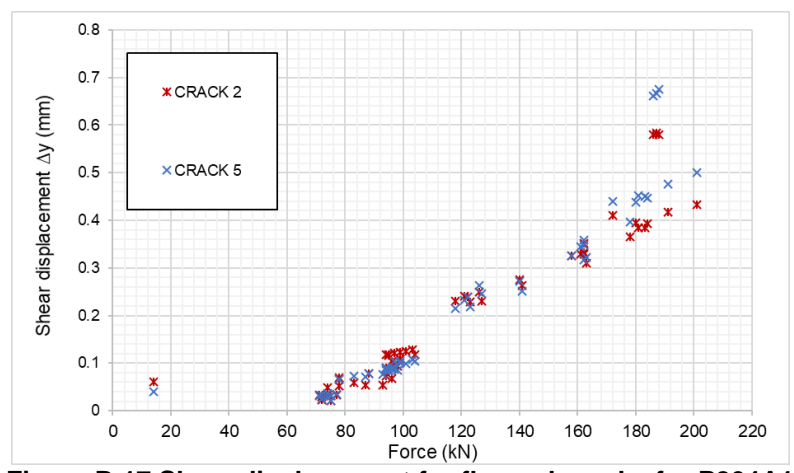


Figure B.17 Shear displacement for flexural cracks for P804A1

It was concluded that cracks 2 & 5 are the critical cracks. In Figure B.18 the red continuous line represents the load step of 180 kN, from which the behavior triggers and is clearly different from the previous steps. The load of 180 kN is equal to 87% of the failure load, at this load level the identified critical shear displacement is equal to 0.4 mm.

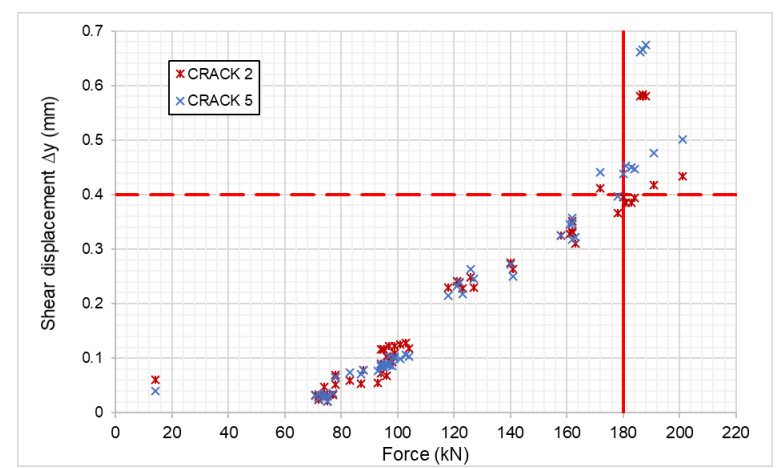


Figure B.18 Critical cracks and critical shear displacement for P804A1

The following figures show the results for crack width vs load. Figure B.19 shows the results for major cracks and Figure B.20 for the secondary cracks. The behavior was as expected, the crack width increases as the load increases and from the load of 160 kN the crack opening seems to stay in a constant value Crack 2 and 5 presented a different behavior.

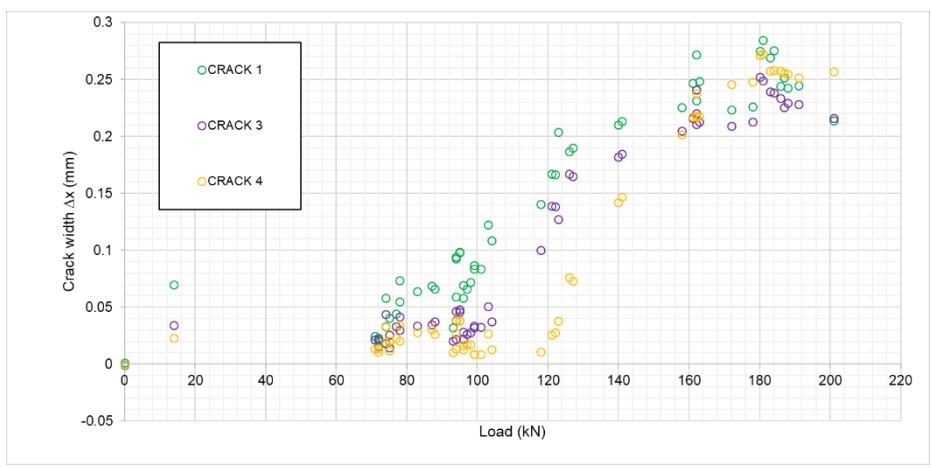


Figure B.19 Crack width for major cracks for P804A1

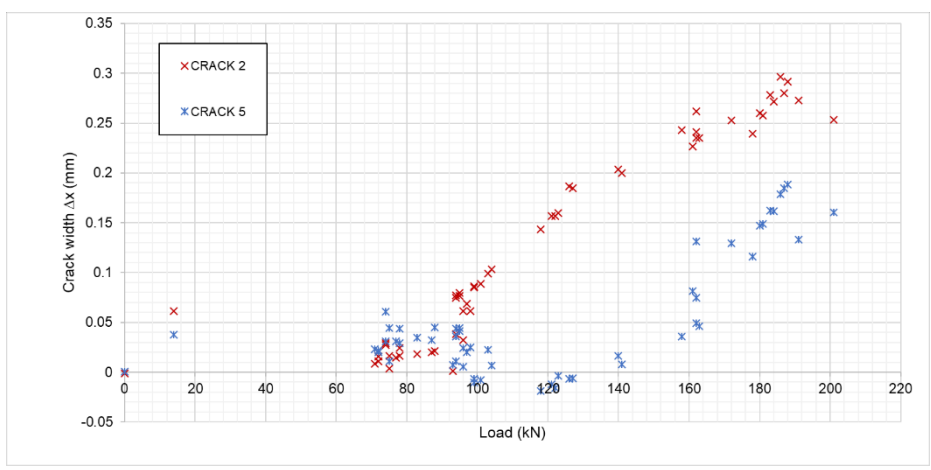


Figure B.20 Crack width for secondary cracks for P804A1

The results of crack width for Crack 1 were analyzed and the crack width identified for the load step of 180 kN was of 0.28 mm. As shown in Figure B.21.

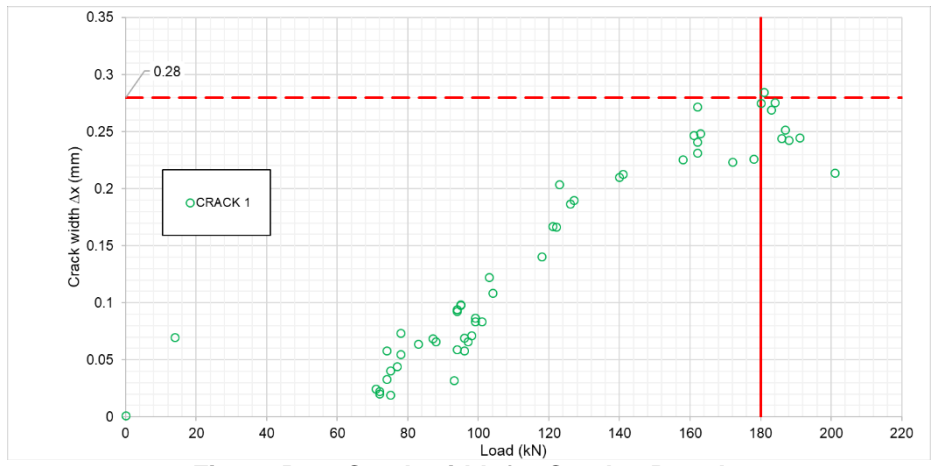


Figure B.21 Crack width for Crack 1 P804A1

## **B.3 RESULTS P804A2**

In total 29 pictures were correlated to obtain the results of the DIC analysis. P804A2 was previously tested in bending. Therefore, the reference image was taken before the test started but cracks already existed.

Test P804A2 fail in shear at a load level of 233 kN.

#### **B.3.1 LOADING SCHEME P804A2**

The loading scheme measured in the experiment and the results obtained for DIC analysis are shown in Figure B.22. The total number of load cycles was 17 and 5 load levels were studied.

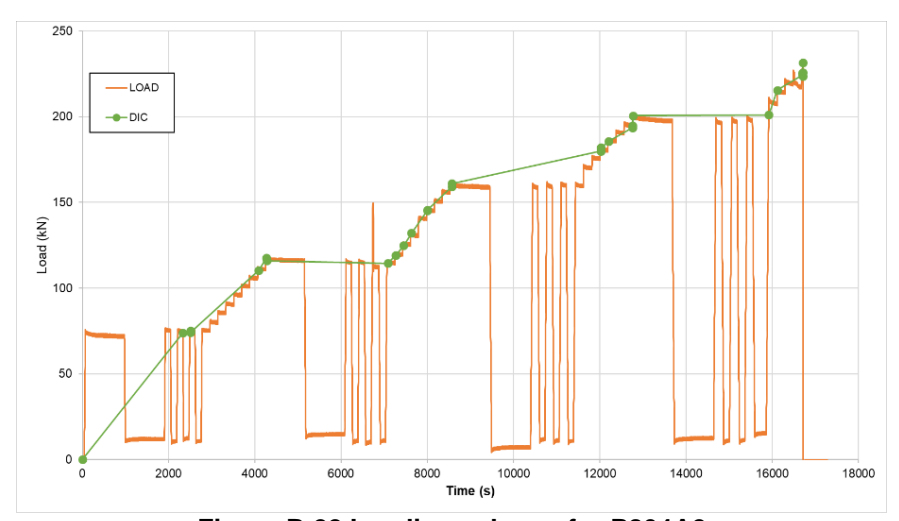
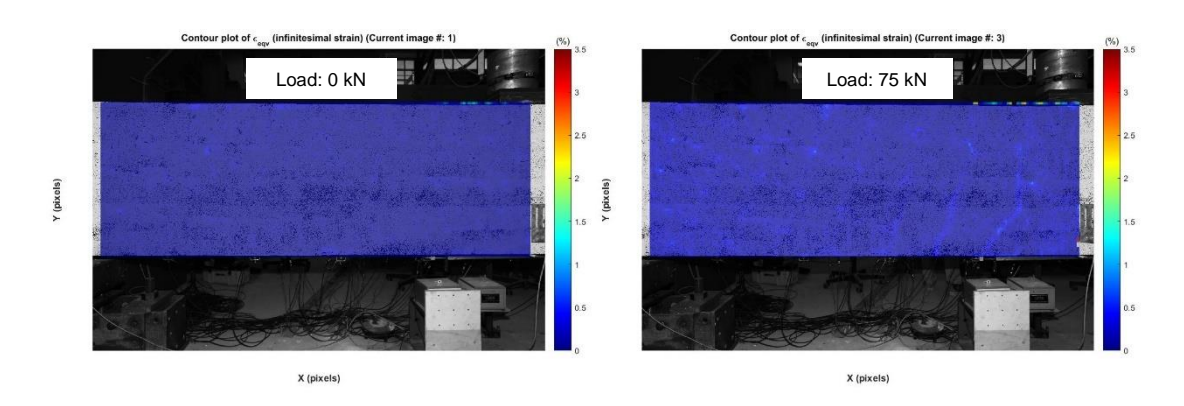


Figure B.22 Loading scheme for P804A2

## B.3.2 DIC RESULTS P804A2

For the DIC analysis, the final subset size used for this group of pictures was of 91 pixels with a grid equal to 30. In Figure B.23, the results for the representative load steps are given.

It can be observed that the first cracks are visible at a load of 75 kN, these cracks are Cracks 3, 4 & 5 from the previous bending test, P804A1. Failure occurs at a load level of 232 kN.



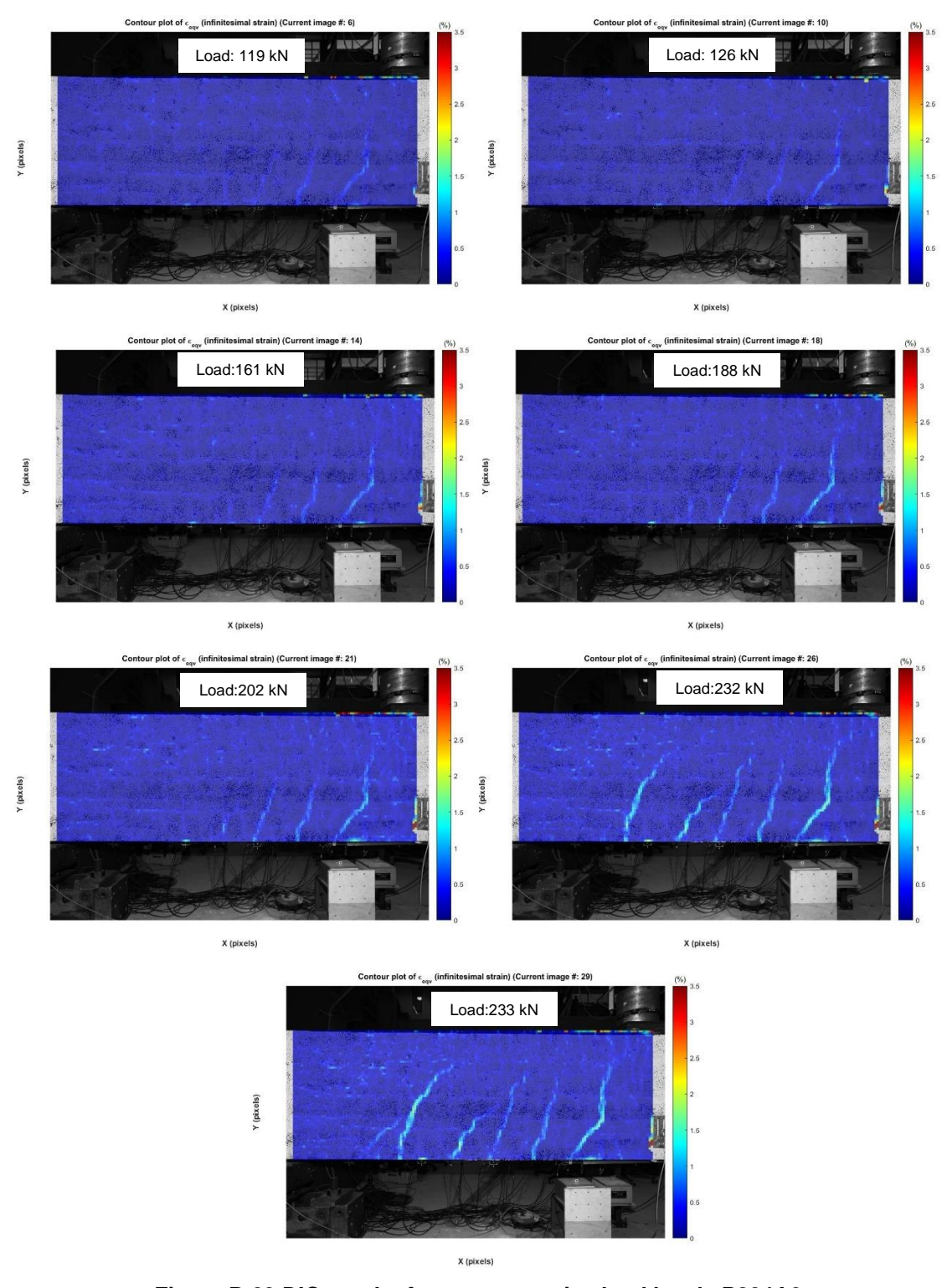


Figure B.23 DIC results for representative load levels P804A2

# B.3.3 MEASURED HORIZONTAL DEFORMATIONS P804A2

The scale for this test was of 0.4447 mm/pix. In Figure B.24, the LVDTs location is shown, as well as the drawn array used for the comparison.

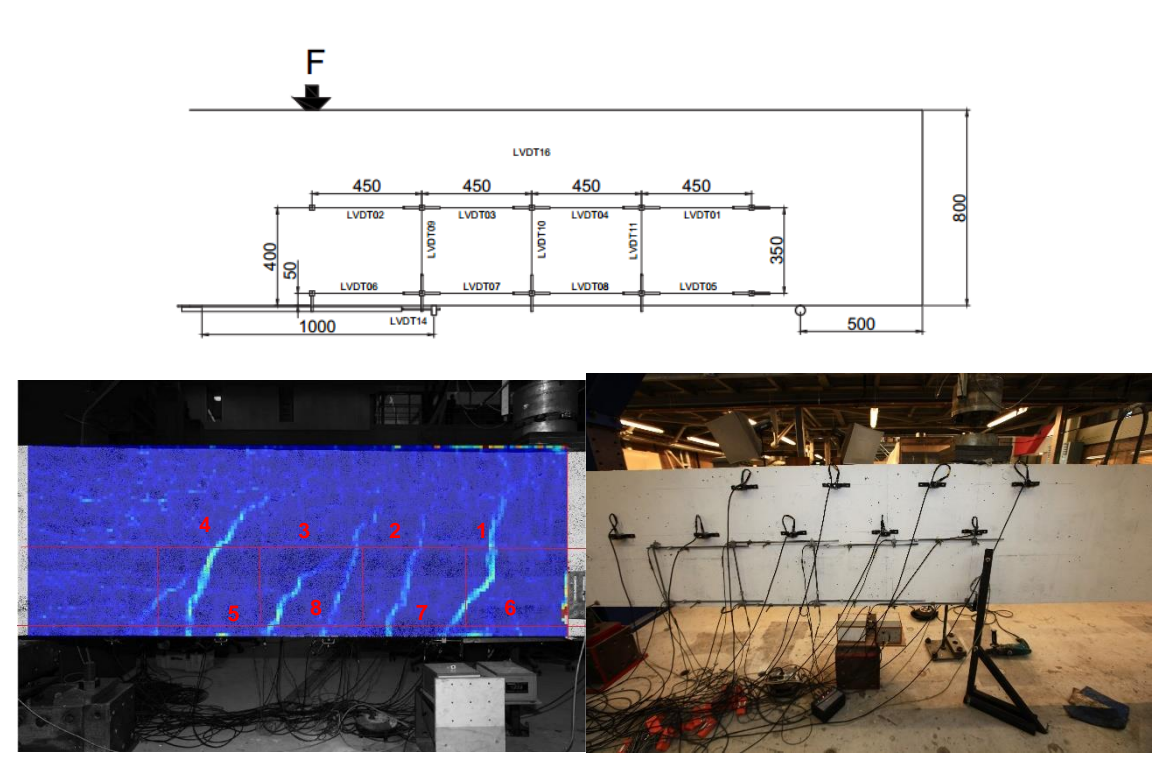


Figure B.24 LVDT array location for P804A2

Figure 44 shows the comparison of the results obtained for the horizontal deformation at the tensile reinforcement level.

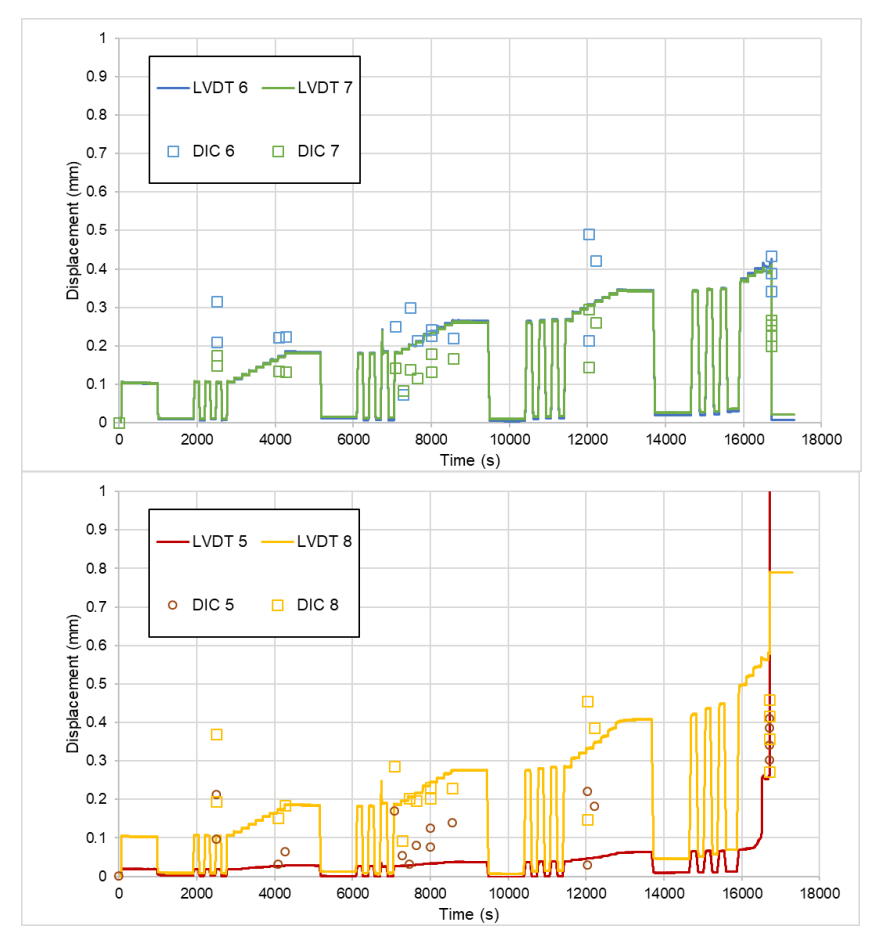


Figure B.25 Comparative of the horizontal deformation development of LVDT's 5-8 & DIC (bottom row) for P804A2

The results of horizontal displacements differ from the LVDTs measurement. However, both results follow the same behavior.

It is important to note that this beam is the same as the previous one, so the same problems with the painted pattern were found, this is a possible explanation for the difference in the results.

# B.3.4 CRACK WIDTH ( $\Delta_X$ ) AND SHEAR DISPLACEMENT ( $\Delta_Y$ ) P804A2

The DIC results for picture 29 were used as background and the reinforcement level was drawn, as it can be observed in Figure B.26.

Four major cracks (1, 2, 3 & 5) and three secondary cracks (4, 6 & 7) cracks were identified (Figure 45).

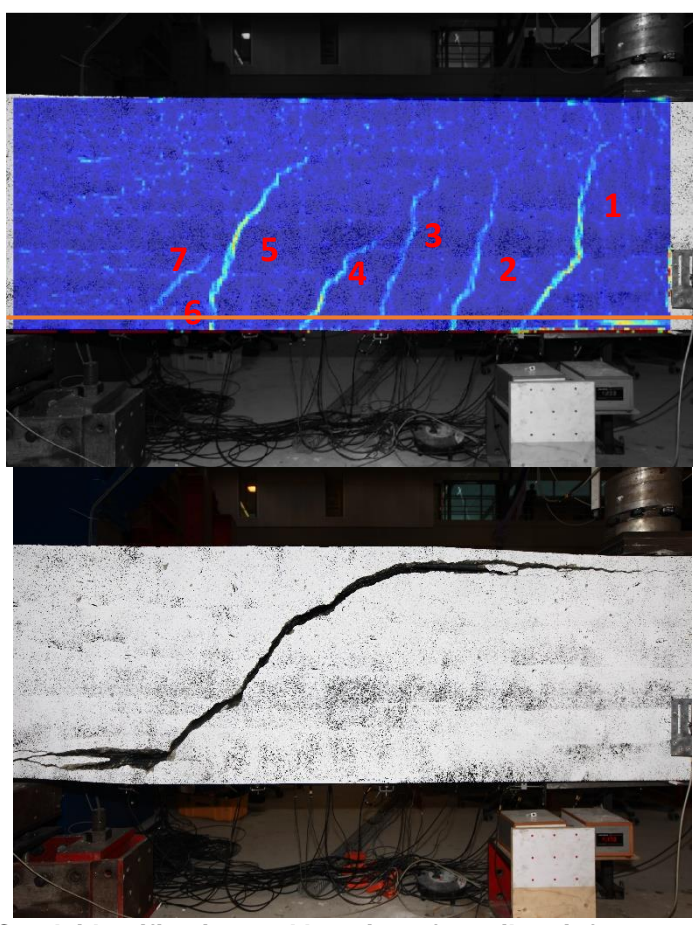


Figure B.26 Crack identification and location of tensile reinforcement for P804A2

The following figures show the plots of shear displacements vs load. Figure B.27 presents the results for the major cracks and Figure B.28, for the secondary cracks. It is important to note that since this beam had already been tested in bending the cracks 1, 2 and 3 already had a displacement.

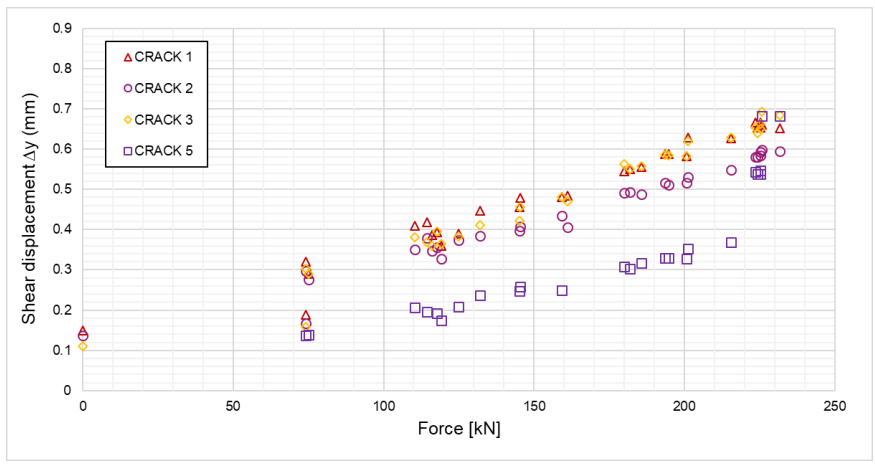


Figure B.27 Shear displacement for major cracks for P804A2

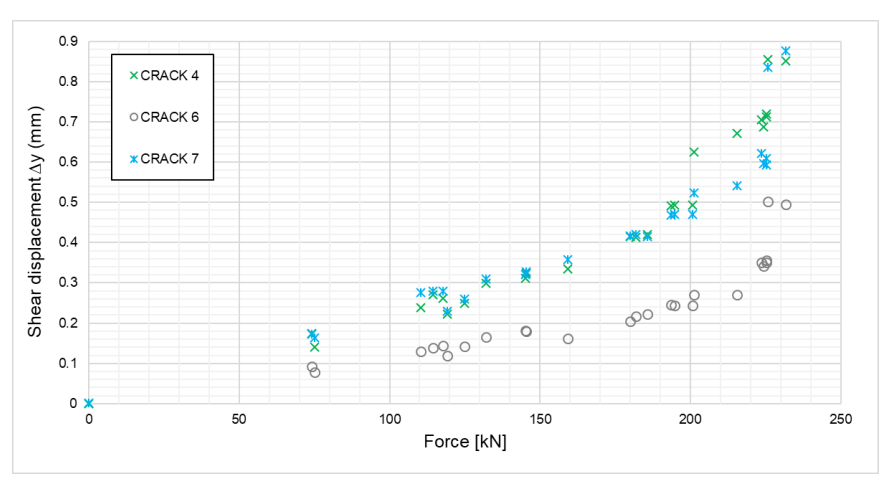


Figure B.28 Shear displacement for secondary cracks for P804A2

After analyzing these results, it was concluded that cracks 4 and 7 are the critical inclined cracks. From Figure B.29, it can be observed that from the load step of 200 kN and onwards the behavior is different from the previous load steps. The red continuous line represents the load level from which the shear displacement triggers, it is equal to the 86% of the collapse load with a critical shear displacement equal to 0.5 mm.

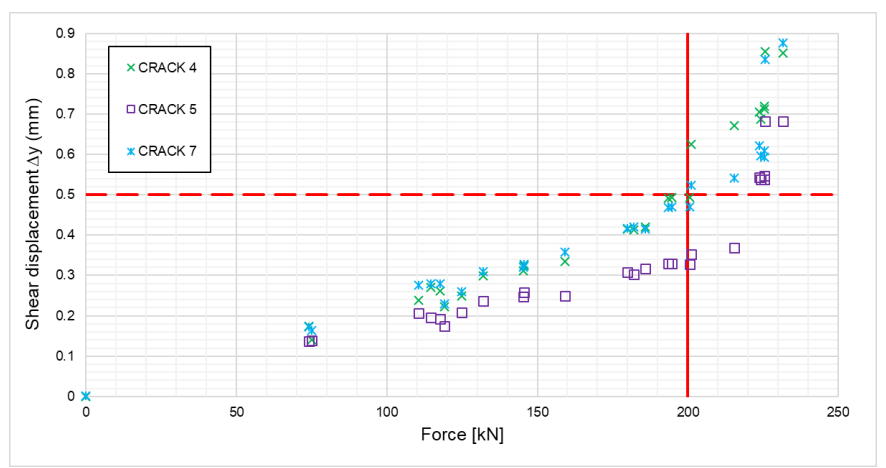


Figure B.29 Critical cracks and critical shear displacement

The following figures show the results for crack width vs the measured load. Figure B.30 presents the results for the major cracks and Figure B.31 for the flexural cracks.

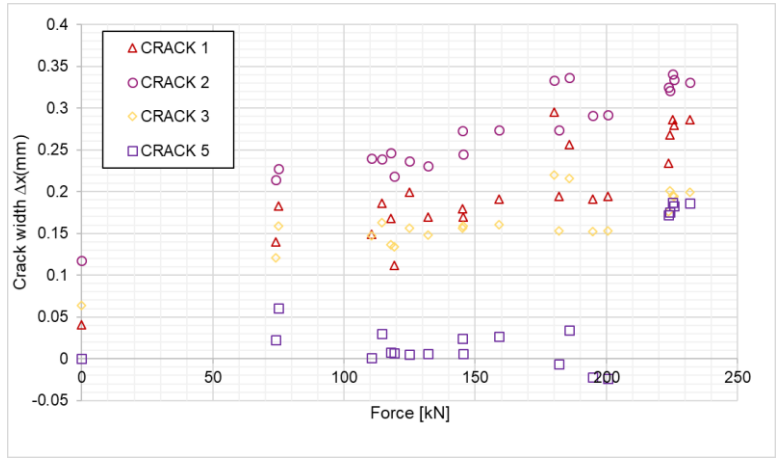


Figure B.30 Crack width for major cracks P804A2

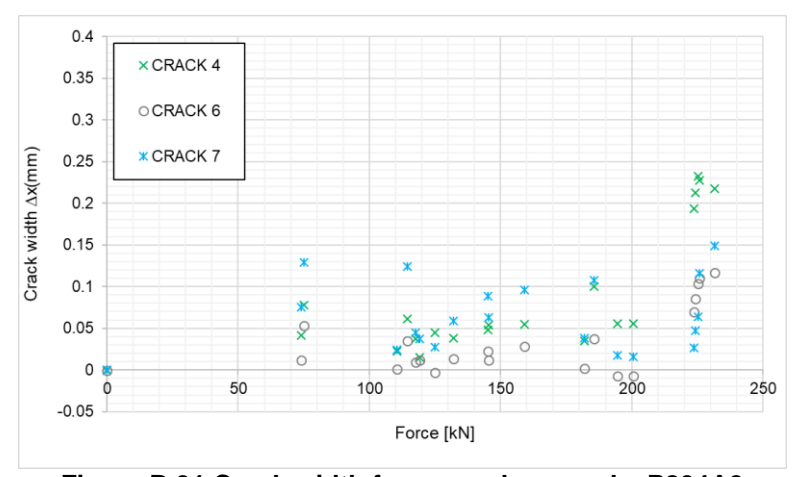


Figure B.31 Crack width for secondary cracks P804A2

The results of crack width for Crack 1 were analyzed and the crack width identified for the load step of 200 kN was of 0.20 mm.

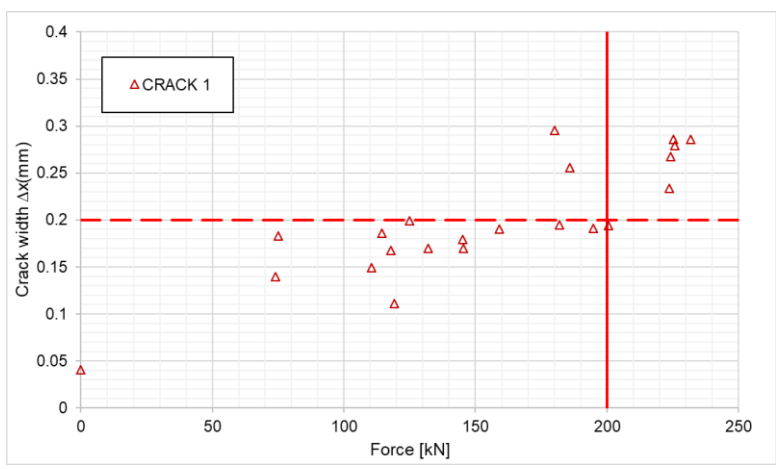


Figure B.32 Crack width for Crack 1 P804A2